Spring 4-23-2020

Learning from Those Who Served: Application of Regression-Based Body Mass Estimation Methods to the USS *Oklahoma* Population

Maxwell Rooney
University of Nebraska-Lincoln

LEARNING FROM THOSE WHO SERVED: APPLICATION OF REGRESSION-BASED BODY MASS ESTIMATION METHODS TO THE USS *OKLAHOMA* POPULATION

By

Maxwell S. Rooney

A THESIS

Presented to the Faculty of

The Graduate College at the University of Nebraska

In Partial Fulfillment of Requirements

For the Degree of Master of Arts

Major: Anthropology

Under the Supervision of Professor William Belcher

Lincoln, Nebraska

April 13, 202

LEARNING FROM THOSE WHO SERVED: APPLICATION OF REGRESSION-BASED BODY MASS ESTIMATION METHODS TO THE USS *OKLAHOMA* POPULATION

Maxwell Steven Rooney, M.A.

University of Nebraska, 2020

Advisor: William Belcher

Current methodologies in body mass estimation are lacking in accuracy when compared to the methods of sex, age, and ancestry estimation familiar to forensic anthropologists. For this reason, the practical application of body mass estimation remains underutilized, hindering the study of a potentially advantageous aspect of the biological profile.

This study highlights body mass estimation in a forensic context while taking the osteological paradox into account through the utilization of a unique population: the US military personnel killed on the USS *Oklahoma* during the Pearl Harbor attack on December 7, 1942. Because these individuals were similar in age (adults, age 18-43 years) and their deaths were catastrophic rather than attritional, it provides an opportunity to control for many variables that other populations cannot. Ruff's (1991) methodology for estimating body mass was applied, utilizing measurements taken from anteroposterior radiographs of the proximal femur and the development of body mass estimation equations via simple and linear regression modeling. These data were cross-referenced to body mass data collected by the US military during the individual's enlistment. The mean squared error of estimate yielded by Ruff's (1991) equations on the sample population

was 104.12 and 62.00 for regression involving femoral head breadth and shaft breath, respectively. This differs from the mean squared error, 81.85 and 59.99, yielded by the equations created for USS *Oklahoma* data. While these results are expected in sample-specific linear regression, the controlled attributes of the sample and the equations produced offer another opportunity through which we can further our understanding of body mass estimation.

AKNOWLEDGEMENTS

First and foremost, I would like to thank my family for their constant support and encouragement in the completion of this project. The countless hours on the phone, care packages, and text messages were integral to keeping me going throughout this whole process. I would also like to thank the numerous academic role models who have provided advice, edits, and guidance to this project: Drs. Bill Belcher, Emily Hammerl, Megan Moore, Brittany Walter, and Sophia Perdikaris; this project would have been lost without your academic expertise. A special thank you to Michael Streyle, whose statistical knowledge and fluency in all things ‘R’ played a vital role in this research. I would also like to thank Emma Olson, whose artistic abilities provided many of the figures in this document.

Additionally, I would like to extend my sincerest appreciation to the anthropologists and staff at the Defense POW/MIA Accounting Agency (DPAA) for not only supplying the CT imaging that made this project possible, but for their constant commitment to research of the highest quality in a supportive and diligent environment. I learned more during my year as an intern/volunteer at the DPAA than I could have ever gleaned from the classroom. I would like to extend a special thank you to DPAA – Offutt Laboratory Director Dr. Franklin Damann for taking the time out of his immensely busy schedule to make sure that this project was completed to the standards that are expected from all DPAA-associated research.

Finally and most importantly, I would like to extend my thanks to the Sailors and US Marines who gave their life serving the United Stated during the Japanese Attack on

Pearl Harbor. More specifically, I would like to thank the individuals who gave their lives on the USS *Oklahoma* and made this research possible.

TABLE OF CONTENTS

LIST OF FIGURES

LIST OF TABLES

LIST OF ABBREVIATIONS

%PE/PPE	**Percent Prediction Error [**(observed – predicted)/predicted]x100
%SEE/SEE	**Percent/Standard Error of Estimate** $\sigma_{est} = \sqrt{\frac{\sum (Y - Y')^2}{N}}$
AGRS	**American Graves Restoration Service**
BMD	**Bone Mineral Density**
BMU	**Basic Multicellular Unit**
CA	**Cortical Area**
CT	**Computed Tomography**
DPAA	**Defense POW/MIA Accounting Agency**
FAR	**Forensic Anthropology Report**
HeadBD	**Head Breadth**
IDPF	**Individual Deceased Personnel Files**
JPAC	**Joint POW/MIA Accounting Command**
MSE	**Mean Squared Error**
NeckBD	**Neck Breadth**
OMPF	**Official Military Personnel Files**
PTH	**Parathyroid Hormone**
ShaftD	**Shaft Diameter**
USS *OK*	**USS *Oklahoma***

Chapter 1: Introduction

From initial missing person reports to the autopsy of unidentified remains, body mass can be an important individuating piece of evidence gathered during forensic investigations (O'Hara, 1973; Eliopulos, 2003). Thus, the estimation of body mass from human remains can be used as a valuable line of evidence for investigators in the identification of unknown remains. However, thus far in forensic anthropology, body mass estimation has been largely understudied as part of the biological profile. One of the greatest difficulties addressed by previous researchers (Ruff, 1991; Moore, 2008) is the lack of controlled samples of individuals from a population with similar, known body mass that would allow testing of various hypotheses regarding body mass estimation. This thesis intends to address the importance of selective sampling and advance body mass estimation from human skeletal remains by: (1) creating unique regression equations for body mass estimation; and, (2) assessing the accuracy of Ruff's (1991) research model using a controlled sample of adult males with similar body mass.

The USS *Oklahoma* (BB-37) was a Nevada-class battleship commissioned in 1916 that served in both the United States Battle Fleet and Scouting fleet. During the Japanese attack on Pearl Harbor on December 7, 1941, the USS *Oklahoma* was struck by enemy torpedo fire, resulting in the 429 catastrophic deaths of 415 US Navy personnel and 14 US Marines. Through multiple salvage attempts, the remains of these personnel were recovered and interred as "unknowns" until the American Graves Restoration Service (AGRS) was enacted in July 1942. Since this time, it has been the mission of US military and civilian personnel alike to identify the remaining unknown individuals from the USS *Oklahoma* through the application of forensic anthropological and odontological methods and genetic testing being completed in laboratories across the United States (Brown, 2019).

Through the utilization of computed tomography (CT), a specialized method of medical imaging that takes a series of thinly sliced X-Rays in order to produce three dimensional digital models, it is now possible to take images of skeletal elements and measure directly from those images with a high degree of accuracy using specialized computer software environments and digital tools. To address the non-specific sampling issue as it pertains to body mass estimation, the proposed thesis research will estimate body mass from skeletal remains and compare these to antemortem information of identified individuals from the USS *Oklahoma* at the U.S. Department of Defense's Defense POW/MIA Accounting Agency (DPAA) Laboratory at Offutt Air Force Base, Nebraska. Specifically, this study will use CT images of skeletal elements, Individual Deceased Personnel Files (IDPFs), Official Military Personnel Files (OMPFs), and/or Forensic Anthropology Reports (FARs) to validate Ruff's (1991) research on body mass estimation. All body mass data will be collected as near the terminal events to account for change in body composition from time of enlistment to the time of death. Due to the daily physical fitness regimen that US military personnel are subjected to, changes in body mass are expected to occur secondary to the addition of muscle mass and the loss of fat mass. Thus, it is likely that data will be most accurate when obtained from regular medical examination during the individual's time served rather than data collected at the time of induction.

The USS *Oklahoma* population is ideal for this study because of the demographic similarity of the individuals in this group. Most of the individuals who died on the USS *Oklahoma* were White males between the ages of 18 to 43 years. As applied in Ruff (1991), a series of four standardized measurements from previously collected CT (previously anteroposterior radiographs) images of skeletal remains recovered from the USS *Oklahoma* will be collected from the proximal femur (superoinferior head and neck breadth – HeadBD and NeckBD; and, mediolateral subperiosteal and cortical breadths). These measurements will then be analyzed via traditional least Squares regression. Once the sample has been regressed and a model has been generated, the results from the USS *Oklahoma* will be compared to the results presented in Ruff (1991) with the aim of cross-referencing the produced body mass estimates with the enlistment body mass for the individual as noted in antemortem documents. The model generated from traditional linear regression will then be evaluated for accuracy through statistical analysis. Particularly, the calculation of mean squared error (MSE) will be used as the primary value for assessing accuracy. The use of body mass estimation as a potential line of evidence for identification will also be assessed. Ultimately, this study will broaden the field's basis of reference knowledge for body mass estimation and potentially provide a means for the DPAA to include body mass estimation in analyses of unknown human remains as another component of the biological profile.

The aim of this particular study is to utilize the methodology outlined in Ruff (1991) and apply it to the USS *Oklahoma* population for means of comparison, but also to use this population to try and gain a better understanding of the variables in the measurements collected (e.g. Shaft Diameter and Head Breadth) and their interactions with one another. This will be accomplished firstly through the creation of a simple linear regression model for head breadth and shaft diameter (described below) in order to generate estimation equations that will be assessed for accuracy and subsequently compared to body mass estimations from equations presented in Ruff (1991). Secondly, multivariate statistical analysis will be applied to assess whether or not there is a significant relationship between any combination of the variables collected. Along with multivariate analysis, this study will more closely investigate two variables, time since measurement and side, to assess whether these variables have a significant impact on the model. Finally, a validation study will be completed for both the simple and statically significate multivariate models through the creating of a training and test set from 80% and 20% of the data, respectively. This will be able to assess overfitting in the model and whether or not the model is suitable for application to additional datasets.

Chapter 2: Skeletal Basics, Current Practices in Body Mass Estimation, & Literature Review

This chapter introduces the basic principles of the human skeleton, analyzes the primary methods of body mass estimation that are being employed in the field of biological anthropology, and discusses the pertinent academic discourse relative to the topic. In practice, the most used methodologies to estimate antemortem body mass can be delineated into two distinct groups, morphometric and biomechanical. Morphometric body mass estimation views the body as a cylinder and estimations are yielded by calculating the volume of the cylinder based on stature and some measure of body breadth. Biomechanical body mass estimation, on the other hand uses the principle of skeletal remodeling and engineering beam theory in order to select different biomechanically related measurements of weight-bearing aspects of the skeleton and apply those measurements to a linear regression model. While each methodology has advantages, at the time of this research, neither have yielded results accurate enough to warrant their application in forensic casework.

Basics of the Human Skeletal Biology

The human skeleton is a complex and hyper-intricate system that enables the daily functions and processes of life. First, the human skeletal system provides structural support and protection for the heart, lungs, and other vital organs. The skeleton also protects other internal organs such as the brain and reproductive organs. The many sulci, tuberosities, and crests located on each bone act as a scaffold for the musculature, allowing for mobility and ambulation. Most notably for humans, our unique skeleton and musculature provides for one of our most unique characteristics as a hominin, bipedalism. Skeletal tissue is comprised of an admixture of collagen, hydroxyapatite, and water with additional small amounts of magnesium, sodium, and bicarbonate. The mineral deposits between these organic compounds account for 99% of the human body's calcium storage and 85% of its phosphorus storage. The calcium stored in this tissue is pertinent because if these stores are not tightly regulated and maintained, the muscles and nerves of the body are unable to function. The skeleton further monitors the body's well-being, as metabolic acidosis triggers a reaction by skeletal tissue to release calcium, maintaining the body's pH level (White et al., 2012: 27).

Bone Synthesis and Remodeling

On a microscopic level, each bone is comprised of a complex system of cells that interact to facilitate bone growth, resorption, healing, and maintenance. The three primary cells involved in this process are known as osteoblasts, osteoclasts, and osteocytes. Osteoblasts are specialized mesenchymal-derived cells primarily located in the periosteum and endosteum. The central role of osteoblasts is the deposition of a material called osteoid. The osteoid that is laid down by osteoblasts forms the matrix that will eventually mineralize and produce new skeletal material. Osteoblasts that are buried in the newly deposited matrix take on a new role in the skeletal tissue, are referred to as osteocytes. These cells are situated in spaces that are known as lacunae and are responsible for bone maintenance and repair. Basic microanatomy of compact bone suggests that inside the osteon, the larger cylindrical structure positioned parallel the axis of compact bone, osteocytes positioned inside of lacunae interact with each other through a series of canaliculi that are situated around a more massive Haversian canal that transects the bone and provides a channel through which blood vessels and nerves travel. Osteoclasts, on the other hand, are derived from hematopoietic progenitors in the bone marrow and primarily break down bone tissue through a process called osteocytic osteolysis. Both osteoblasts and osteoclasts act in union with each other to regulate the rate at which new skeletal tissue is deposited and resorbed while osteoclasts work to maintain it and subsequently respond to stress or fracture. This cooperation, in turn, regulates the rates at which the bone is able to regenerate and respond to various forms of strain (White et al., 2012: 37). As such, the largest voluntary load applied to bone on a day to day basis comes from the muscles that are directly attached to them. Schiessl et al. (1998: 1) describes that the areas where bone is strengthened, reinforced, modeled, or remodeled is determined by strain thresholds which can have a direct impact in that elements' morphology. Thus, an expansion to Wolff's Law was proposed for osseous material in 2001, which was deemed the Utah Paradigm. This constitutes a continually evolving paradigm of skeletal physiology that combines tissue-level and anatomical features with older ideas which emphasized cell-level features and roles (Frost, 2001).

There are two vital propositions made by this paradigm: 1) that healthy, postnatal load-bearing bones are designed to have only enough strength to keep chronically subnormal, normal, or supranormal voluntary loads (not injuries) from causing spontaneous fractures. The second preposition 2) is threefold, firstly, that in order to achieve mechanical competence, bone's tissue-level mechanisms need nonmechanical factors and effector cells (osteoblasts and osteoclasts); second, in a negative feedback arrangement, bone loads and strains guide those biologic mechanisms in time and anatomic space; third, that most nonmechanical factors can help or modulate that guidance but cannot replace it (Frost, 2001: 399). According to this paradigm, remodeling is determined by Basic Multicellular Units (BMU's) that are working in response to either mechanical (biomechanical strains and stresses) or nonmechanical (hormones, dietary calcium, gene expression, age, ancestry, sex) factors (Frost, 2001: 401).

Basics of Skeletal Biomechanics

One of the reasons that skeletal tissue is so unique from epithelial, muscular, and nervous tissue is because of its ratio of organic to inorganic components (Currey, 2002: 4-5). Since more than 65% of bone is inorganic and comprised of hydroxyapatite with other trace minerals, bones are rigid and able to act as the scaffold on which the rest of the bodily systems operate. Despite this rigidity, the cells through which the organic components of bone further interact for the tissue to repair the stress and strain of an individual experiences in their daily life. In principle, when large or recurrent amounts of stress are applied to a bone, microfractures form that corresponds to the pressure applied. The bone then undergoes a complicated method of healing in which a unique pre-bone material known as osteoid is systematically deposited and resorbed, reinforcing the area where stress was applied. This remodeling changes the cross-sectional geometry of the bone when viewed from the transverse plane. In most cases, the bone will strengthen at areas of principal strain (Corwin, 2001; Frost, 2001). For instance, axial compression applied to long bones results in a generally thicker cross-section. While certain types of stress and strain have been shown to have an impact on the cross-sectional geometry of a bone, this is not the only influencing factor. Another would be the genetic makeup of the individual being analyzed. This is evident in the variation that can be seen in the morphologies of same-sided elements from individuals of the same sex, age, geographic location, and population (Corwin, 2001).

Types of Biomechanical Force

Before the different ways in which forensic anthropologists attempt to estimate antemortem body mass from skeletal elements are examined, it is first essential to understand the various forces that a human long bone endures during an individual's life. Most of the stress applied to bone can be categorized into five types of loading: compression, tension, shear, torsion, and bending (Currey, 2002). Compression occurs when force is applied to both ends of an element and creates pressure on both ends simultaneously. Aside from gravity, in the human skeleton, compressive force is a result of weight support and external carrying or loading. The next simple type of force loading applied to a bone is tension. Tension occurs when two forces pull or stretch a skeletal element in opposite directions. Due to the basic principles of gravity, the human skeleton is much less resistant to tensile forces than it is to the final type of simple loading, shear. Shear force refers to when two forces are acting in parallel, but two directions are applied to the bone, and the two aspects are displaced relative to the other. A simple example of shear force is when an individual is skiing down a hill and the foot affixed to the ski stops abruptly. Although the ski and the foot cease to be in motion, the rest of the body is propelled forward at an equal speed to which it was traveling prior.

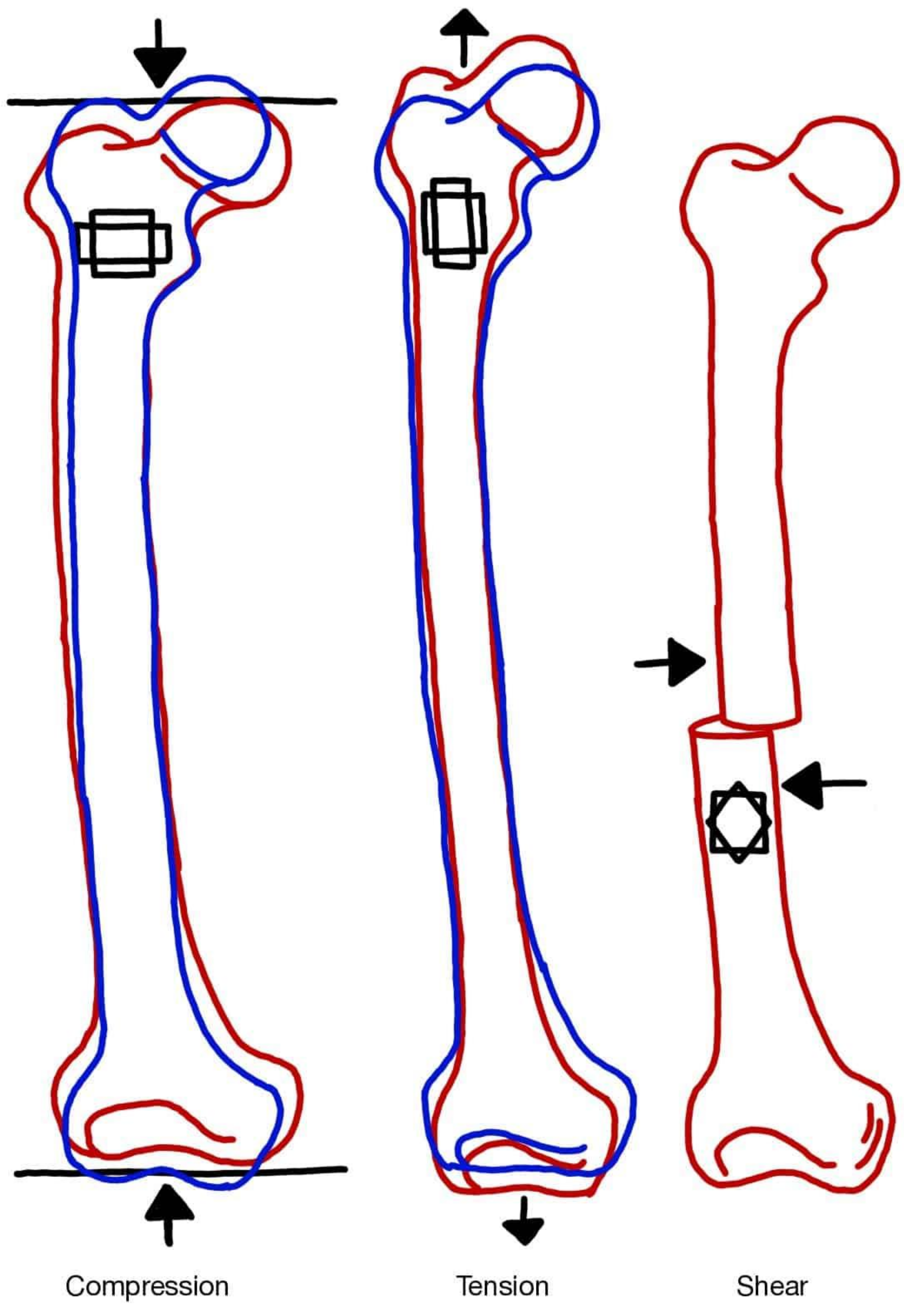

Figure 1: Types of simple loading on a human long bone. The square inside the femur and blue illustration represent the element prior to loading, the rectangle or diamond shape and red illustration represent the element after loading. The black arrows represent the directionality of the forces applied.

Unlike the simple types of loading above, torsion and bending are more complex as the type force being applied to the bone results in a combination of different types of loading. Bending, as it sounds, is force applied to an area that has no support from the framework (Figure 2). Imagine the action of bending a stick in half. The forces being applied to the stick results in an admixture of tensile strain on the convex side and compressive stress on the concave. Most often, bending forces to bone results in failing on the side of the tensile strain as bones (especially long bones) are less resistant to tensile forces than they are to compressive forces. Torsion, on the other hand, or rotational force refers to twisting along the bone's longitudinal axis (e.g. grasping a ruler on both ends and twisting in opposite directions) (Figure 2). Torsional strength applied to bone can result in stress applied to both perpendicular and parallel to the axis of the bone. Torsional loading can additionally occur in intensive and compressive strengths at the angle of the structure (Choi and Goldstein, 1992) (Figure 2).

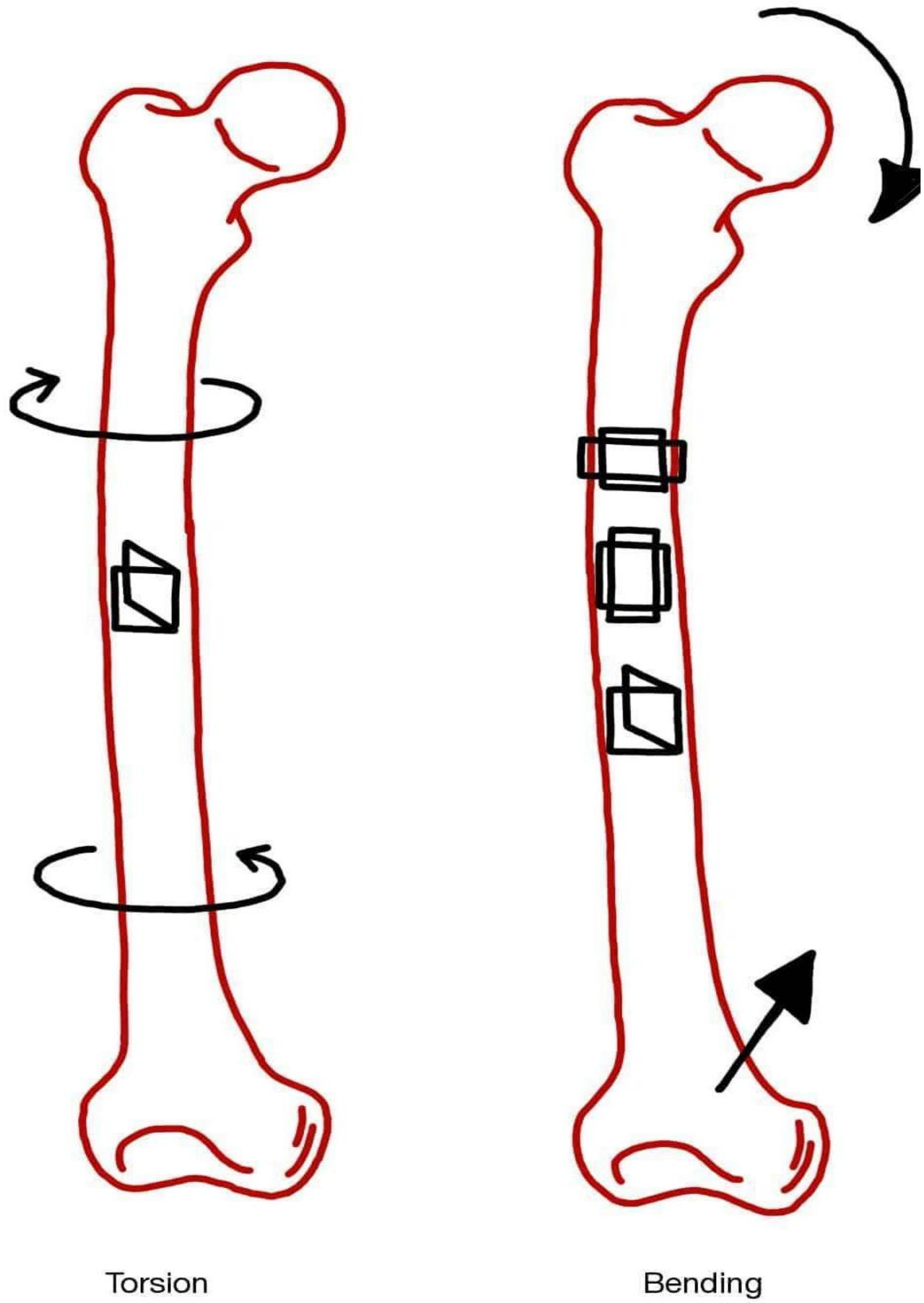

Figure 2: Types of Complex Loading on a Human Long Bone. The square represents the element prior to loading and the rectangle or parallelogram represents the element after loading. The black arrows represent the directionality of the forces applied.

Confounding Variables in Bone Strength

One compounding variable in total bone strength is the shape of the bone and the ratio of cortical to trabecular bone that the element is comprised of. This influences the types of forces to which the element is most resistant. For instance, long bones such as the femur are most resistant to axial compression than the bones of the cranium that are more resistant to the application of outward force secondary to their unified globe shape (White et al., 2012: 241). One example of this principle would be the articular surface of the knee joint in athletes who more regularly place strain on their muscles, and subsequently, the bones they are attached to, than their non-athlete peers (Eckstein, 2002: 46). Thus, to some extent, bone is shaped by activity level, which is uniquely displayed within the affected bone's cross-sectional geometry (Kennedy, 1989; Lai and Lovell, 1992).

While the types of forces applied to bone and the frequency of those forces applied to it affect its cross-sectional geometry, the cross-sectional morphology of a bone is also influenced by other factors such as sex, age, diet, hormone levels, and environment. Additionally, the ways in which bones respond to stress and fracture are similar in males and females, the subtle morphological and microscopic differences between biological sexes can play a significant role in the bone's mineral composition (bone mineral density) as well as its overall response to stress. One study (Kirchengast et al., 2001) found there to be an association between low amounts of fat tissue and increased bone mineral density (BMD) in women that could be the result of reduced conversion rates from androgens to estrogens in a small amount of adipose tissue. Additionally, Lacoste et al. (2018) observed differences between the ratios of fat mass, fat-free mass, and body mass percentage for men and women, respectively. The authors (Lacoste et al., 2018: 1) found that "..[t]he observed sexual dimorphism is consistent with differing aging processes; cortical bone decreases in females through endosteal resorption while it remains almost constant in males who compensate for endosteal resorption by periosteal apposition on the diaphyseal surface".

Age also influences how the skeleton responds to stress. For most humans, the skeleton is not fully mature until approximately age 25 (earlier for females and later for males). During this time of development, bones are significantly more plastic and responsive to stress. The response of a juvenile skeleton differs from the reactions of the adult skeleton because of increased mineralization in the diaphysis and fusion at the epiphyses, creating a much more rigid tissue (White and Folkens, 2005: 363). While a more mineralized bone may be more resistant to bending forces, this places the tissue at a higher risk for fracture as the bone is less plastic. This problem of rigidity and stiffness is further affected by the degenerative processes that the skeleton undergoes as it ages, such as osteoporosis and osteoarthritis (White et al., 2002: 384).

The vitamins and minerals in an individual's diet can also have profound effects on the skeleton. It is a commonly understood that the calcium absorbed from food reinforces the bones of the body (Snoddy et al., 2018). A lack of vitamins in an individuals' diet can lead to diseases such as scurvy. Individuals with scurvy have bones that lack the proper level of collagen due to lowered levels of Vitamin C and, as a result, the capillaries in the bone release excess blood. This signals osteoblasts to deposit osteoid overtop the already formed skeletal tissue, thus creating pathological lesions to the affected bone. This bleeding often pools underneath the periosteum and causes severe pain for individuals suffering from this deficiency (Snoddy et al., 2018).

Another type of regulator of bone strength and shape is an individual's hormone levels. First and foremost, parathyroid hormone (PTH) plays a vital role in bone calcium maintenance, resorption, and formation. If calcium levels in the body are low, the parathyroid gland releases PTH, which indirectly promotes osteoclast activity and raises serum calcium levels to maintain homeostasis. Likewise, if calcium levels are high, the parathyroid ceases release of PTH and encourages the storage of calcium to reach equilibrium. An additional unique and vital hormone that is synthesized by the human body from diet/environment and regulates bone health is Vitamin D. Vitamin D is one of one vitamin that the human body is only able to produce when exposed to UV light, but it remains vital to skeletal wellbeing. Without Vitamin D, the body would not be able to metabolize calcium and phosphorus efficiently. As an example, children who worked in factories during the Great Depression could not get the necessary amounts of Vitamin D to effectively metabolize minerals from their diet and eventually developed rickets, a pathology where the mineral matrix of a developing skeleton is compromised due to deficient mineral levels. This causes the weight-bearing bones to collapse in on themselves, causing the disease's trademark 'bow-legged' morphology (Mays et al., 2006).

Engineering Beam Theory

Because of their biomechanical properties, each of the long bones in the body can be modeled as beams. It is possible to analyze the effects of different biomechanical strains to bone using engineering beam theory. As has already been established above, each bone is subject to various forces that often act simultaneously and congruent with each other. Along the same lines, skeletal remodeling is also anisotropic in nature, meaning that it is directionally dependent and three-dimensionally responsive (Ketcham and Ryan, 2004). These are two of the primary reasons that the forces being applied to bone are so difficult to model mathematically. Polar moment of inertia is a measure that assesses the torsional strength of bone, stating that torsional strength is directly related to the distance of the strain from the neutral axis, or the axis of the shaft with no longitudinal stressors or strains. Most often, this neutral axis refers to a line running through the center of a long bone's medullary cavity. The closer the force is to the neutral axis, the less resistant it is to torsional strain. One way to measure bending strain in bone is through the area moment of inertia (Moore, 2008: 19). To understand this, Larsen (1997) offered the analogy of a ruler. If one attempts to snap a ruler in half along its width, it fails quickly; the ruler is much more resistant to bending when trying to bend it along its linear axis.

This same analogy is applicable when attempting to understand the human femur. Just as the ruler analogy, human femora are much more resistant to forces acting near the neutral axis such as compression, and much less resistant to those forces that act transverse to the femoral diaphysis. Because bone is a plastic tissue and can heal and remodel, this kind of beam theory is integral when understanding how the element reacts in response to stress and ultimately how it remodels. In reference to the femur, and before beam theory can be applied, it is important to understand that the forces acting upon the femur are also influenced by the articulating joints, tendons, and bones. This means that in practice, many of the problems occurring in orthopedic biomechanics are statistically indeterminate. As a simple example, the load transmitted to the femur is controlled by both the articulating points of the os coxa as well as the distal elements of the tibia and fibula (Salathe et al., 1987: 189). This must be considered when attempting to estimate body mass because while beam theory is applicable to forces acting directly upon the femur, like sheer force applied transverse to the femoral diaphysis, nearly all compressional load will be informed by the elements to the superior and inferior. As far as beam theory is considered when it comes to long bones like the femur, most research regards them as a curved, three-dimensional beam in which the cross-sectional properties vary continuously along its length (Salathe et al., 1987: 190).

Morphometric Body Mass Estimation

Currently, there are two primary ways in which anthropologists are attempting to estimate antemortem body mass, morphometric and biomechanical methodologies. The first of these methods, as its name implies, utilizes a morphometric approach. This approach views the body as a cylinder, and quite simply attempts to estimate antemortem body mass by first accounting for the non-skeletal tissues of the body, a strategy that can be problematic (Shaw, 2010), and then applying a measure for height (stature) and some measure of body breadth (Ruff et al., 1994: 72) to calculate the volume of the cylinder. Bi-iliac breadth or possibly some interclavicular measurement has been shown as a good measure of body width (Moore, 2008; Ruff et al., 1994). Finally, after both body height and breath are accounted for, these measurements are input into an equation to calculate the volume of the cylinder. While this method of body mass estimation is highly effective when addressing questions such as adaptation to environmental strains (Ruff, 1991; Ruff and Walker, 1993) or questions discussing Bergmann and Allen's rules (Allen, 1877; Bergmann, 1847), it becomes problematic when attempting to estimate body mass of individuals from specific populations. Ruff (2000) showed that when applying bi-iliac breadth to this methodology, it tended to underestimate males by 3% and overestimate females by 3%. Because morphometric body mass estimation assumes that the body is cylindrically proportional, this method is highly inaccurate when attempting to estimate individuals who are extremely under/overweight (Moore, 2008: 2).

Biomechanical Body Mass Estimation

Aside from the morphometric approach to body mass estimation, an alternative method is considerably less theoretical. This method utilizes actual populations by collecting measurements of a biomechanically-related element, plotting those measurements against an individual's known antemortem body mass, and then creating a 'line of best fit' for the data. After this line is created, it becomes possible to estimate the body mass of an individual based on the body mass and measurements of the population initially studied through the utilization of simple linear regression (Moore, 2008; Ruff et al., 1991). While this method of body mass estimation is certainly more population-specific and perhaps better suited for forensic application, it is not without shortcomings. As mentioned earlier, the different forces applied to bone very literally shape its cross-sectional geometry (Moore, 2008). This factor, compounded by the fact that because every individual experiences a varied diet, level of physical activity, and level of hormones, leaves many “unchecked” variables that could quite possibly skew results. Results which are further skewed by individuals who are genetically different which could lead to a series of differences to be discussed below. It is for this reason that the present study aims to investigate this issue through its application of a uniquely ‘controlled’ sample, the USS *Oklahoma* population.

Because the bones of the lower extremities are the primary weight-bearing elements for bipedal humans, it reasonable to assume the lower limbs should be used to examine body mass. Much of the variation in methods for body mass estimation comes when referring to which features, and measurements of the lower limb bones are utilized for further study (Auerbach and Ruff, 2004; Ruff, 1991; De Groote and Humphrey, 2011). Many researchers have selected the femora (particularly the proximal end) to measure as the most significant component to correlate an individual’s body mass with skeletal morphology (McHenry, 1992; Moore, 2008; Ruff, 1991).

The Osteological Paradox

One of the problems that this research hopes to combat is known as the “osteological paradox,” which states if we can physically view a human skeleton, there is an underlying reason or pathology behind why. In other words, there are reasons why this skeleton became part of the collection we are examining. Wood et al. (1992) posits that before we begin to consider a specific skeletal sample, we must account for, “…three important conceptual issues - demographic nonstationarity, selective mortality, and hidden heterogeneity in risks..” that can “…render inferences based on various demographic and epidemiological measures meaningless”. Firstly, by demographic nonstationarity, the authors refer to the fact that a population is continually changing as new individuals leave and other individuals are born or immigrate into the population. Selective mortality refers to the fact that the individuals that make up any skeletal series are dead, and thus the sample does not depict all the individuals who were at risk of death at a certain age but died later due to variation in frailty. Quite possibly, a 60-year-old in any given skeletal collection could have been deathly sick at the age of 20 years but survived to live another 40 years due to the individuals robusticity (Wood et al., 1992: 344-345). Finally, the last and most pertinent aspect of the osteological paradox to this study is that of hidden heterogeneity in risks. This maintains that every skeletal sample is made up of an unknown admixture of individuals who were variably susceptible to pathology and consequential death. Excluding obvious trauma, it is difficult to definitively state a cause and manner of death for every individual in a skeletal collection.

There are a variety of reasons that the osteological paradox is pertinent to body mass estimation, but the most glaring is the fact that body mass is closely linked with mortality. Much like age, the body mass of an individual can be a direct factor in overall health. In modern populations, this is evident by cardiac diseases such as hypertension, diabetes mellitus, coronary pulmonary artery disease, and congestive heart failure. The difference between the relationship between age and mortality in comparison to body mass and mortality, though, is while age is a constant progression that happens at the same rate for each individual, body mass can fluctuate throughout an individual’s life. Often this means that one person will have phases of being relatively different weights throughout their lifetime. As stated above, because body mass is one of the most inconsistent aspects of the biological profile, to produce more accurate estimations in body mass, we must attempt to utilize reference samples that can control for variables such as age, fitness level, and pathology.

This study attempts to account for the osteological paradox in two primary ways. First, this study uses a homogenous population of similarly aged white males who are healthy and of relatively similar weights. Secondly, this sample is drawn from a population of individuals who perished in a catastrophic event. In short, the individuals who died on the USS *Oklahoma* did not die as a consequence of their health, but in a traumatic event.

Body Mass Estimation in Paleoanthropology

One subfield of biological anthropology that utilizes body mass estimation is in Paleoanthropology to estimate the body mass of *Homo sapiens'* hominin ancestors. McHenry (1992) developed one of the most widely known methods of hominin body mass estimation. This study was conducted on a collection of 66 relatively modern human skeletons that varied in origin and size to simulate the variation seen in the fossil record. This methodology involved measuring 13 different postcranial elements. Subsequently, the author created 78 regression equations to be used to estimate all species in the hominin line. One proposed issue with this method of estimation is that there is no absolute antemortem body mass data, so in fact, this method of estimation is based on estimation.

Unlike McHenry (1992), Ruff (2000) used body mass information from Olympic athletes and compared their body size to that of hominids. While this sample did not include any modern humans, Ruff (ibid.) applied these data to a morphometric body mass estimation method and regressed body mass against the variables of bi-iliac breadth and stature. The reason that this body mass estimation method is useful for Ruff (ibid.) is that it "…applied to skeletal samples where stature can be estimated, and bi-iliac breadth is known or can be estimated" (Ruff ibid.: 508). As stated above, this body mass estimation method proved to underestimate body mass in females and overestimate in males, but Ruff (ibid.) also maintains that these equations utilizing bi-iliac breadth and stature could apply to modern populations in settings where stature is well accounted for.

Skeletal Body Mass Estimation

While nearly all of the methods of body mass estimation that utilize medical imaging technology are biomechanical in nature, many of the methods applied to physical bone are morphometric. Baker and Newman (1957) were at the forefront of researchers attempting to quantify the relationship between skeletal mass and the antemortem body mass of an individual. This research comes from bioanthropology and forensic anthropology, where researchers began to apply their knowledge to the identification of human individuals. The authors suggested that the methods being implemented "…do not provide the desired certainty for the identification of an individual" (Baker and Newman, 1957: 601), but they also suggested body mass estimation could be a crucial piece of evidence when attempting to identify unknown individuals. Through the systematic body mass measurements of 125 skeletons of White and Black males, the authors stated that the mineral aspect of bone accounts for 5-7% of the total fat-free body mass. Baker and Newman's (1957) study laid the groundwork for the academic discourse that begot this subfield of study.

Because the talus is one of the primary weight-bearing bones in the human body, Huxley (1992) examined its morphological features to assess the correlation of these measurements to body mass. Her sample was comprised of 88 individuals with body mass data from three skeletal collections. After the author collected 21 measurements from 49 right tali, she concluded that there were no correlations between any of the variables she assessed and antemortem body mass (Huxley, 1992: 36). This statement was fueled by the fact that when analyzed, the correlation between talar morphology and body mass was a low adjusted R-squared value of 0.21.

Wheatley (1999) and May (1999) both examined the relationship between bone mineral density and antemortem body mass. Wheatly noted correlations between body mass and bone mineral density by assessing a sample of 42 living individuals using an X-ray bone densitometer. This tool takes a radiographic measurement of the mineral density of a skeletal element and, in the medical field, it is most often used to detect osteopenia or osteoporosis. Wheatley (ibid.) collected measurements of the femoral bone mineral density, the minimum diameter of the femoral neck, and shaft breadth inferior of the lesser trochanter and found a correlation between the femoral variables collected and antemortem body mass. May (1999) demonstrated a similar correlation through a sample of 73 skeletons from the Smithsonian's Terry collection. In this study, measurements of bone density were regressed against the individual's known antemortem body mass to show that this feature can be used to predict body mass with at least as much accuracy as other body mass estimation methods at the time. May (1999) also determined that the most representative element for density measurements is the fifth lumbar vertebra.

Sichta (2000) examined 189 skeletons from the Smithsonian's Terry Collection to understand the differences, per Wolff's law of bone remodeling, between the skeletal elements of the upper and lower extremities. To do this, the author collected three measurements from the humerus and femur (proximal, midshaft, and distal). The goal of this study was to examine the indices and differences of analogous measurements from the humerus and femur (Sichta 2000: 29) based on the hypothesis that the humerus is modeled in relation to the femur. By identifying the differences in the humeral and femoral measurements, the author highlights that a higher amount of differentiation in the measures of the upper and lower extremities could suggest a person of increased or diminished mass, respectively. Sichta (2000: 67) showed a correlation between antemortem body mass and the measurements of the humerus and femur. However, he was unable to produce regression equations for body mass estimation with an estimated interval that was too large to be of use to forensics.

Because the cranium is frequently the only element found *in situ* in forensic anthropological and paleoanthropological context due to the numerous taphonomical processes, Stubblefield (2002) broke away from a hypothesis grounded in weight-bearing elements. She attempted to examine the correlation between the features of the cranium and antemortem body mass. Her sample consisted of 147 total adults with known bodyweight (mass) information from both the Smithsonian's Terry Collection as well as modern Florida autopsies. From this sample, she collected 16 ectocranial measurements along with seven measurements of cranial vault thickness. By comparing the cranial measurements to the known body mass data, Stubblefield (2002: xi) concluded that they were "…largely unsuitable for bodyweight prediction".

Moore and Schaefer (2011) assessed the bone mineral density of the proximal femur and utilized three-dimensional bone surface models from computed tomography (CT) imaging to estimate antemortem body mass from the human skeleton. Through the collection of many of the same variables as Moore's (2008) study, the authors produced a regression tree that was able to account for missing variables along with continuous variables that do not enter the model linearly while simultaneously creating meaningful divisions within the data and accommodating categorical and continuous parameters. By using this regression tree, the estimations yielded confidence intervals as low as ±17.1kg (Moore and Schaefer, 2011: 1119).

Like Stubblefield (2002), De Groote and Humphrey (2011) sought for a correlation between the first metatarsal, an element often found *in situ*, and antemortem body mass. The sample was comprised of 87 skeletons varying in size and ancestry but without any absolute antemortem body mass data. These individuals were representative of a wide range of both size as well as geographic location (35 individuals from the United Kingdom, 9 unspecified African individuals, 21 Andamanese, 7 Australasians, and 5 Native Americans from Santa Cruz - USA). Subsequently, four measurements were collected that were regressed against body mass. This method was able to prove a significant correlation between the first metatarsal and the femur, most notably the relationship between dorsoplantar diameter and femoral head diameter ($r = 0.911$) (De Groote and Humphrey, 2011:627). Regression equations from this study yielded Percent Standard Error of The Estimates (%SEE) of less than 4-7.19%. This means that the model was able to estimate body mass with an error of 4-7.19% of body mass as presented in kilograms.

Radiographic Body Mass Estimation

To develop methods of body mass estimation based on living populations, researchers have utilized measurements from living individuals. First, and most applicable to the research for this study, is Ruff et al.'s (1991) method of biomechanical body mass estimation that used anteroposterior radiographs to measure the femoral dimensions of 80 individuals. This population varied in age from 24-80 and was comprised of approximately 2/3 individuals of European ancestry and 1/3 individuals of African ancestry. These measurements subsequently were plotted, and regression equations were created for means of body mass estimation. In conclusion, this study was able to predict body mass within a 10%-16% average percent error for the reported body masses of individuals in the sample. In order to account for this percent error, Ruff et al. (1991: 406) state that body mass estimation in humans remains difficult task "…because of problems obtaining sufficiently accurate body masses individually associated with skeletal remains in a large, random, and representative sample". The problem being highlighted by Ruff in this statement is one that has already been stated above. The problem of finding a sample of random individuals that are nonpathological with accurate measurements of body mass near the time of death is a constant limiting factor in body mass estimation from skeletal material. This is compounded by morphological and genetic differences between individuals that could possibly skew results and complicate estimation.

Similarly, Sciulli and Pfau (1994) use the femoral dimensions from radiographs of 183 children in central Ohio. Femoral diameter, defined as a measure of the diameter of the femoral shaft, was regressed to each individual's mass. The authors were able to accurately account for 90-96.8% (R-squared value) of the variation in body mass using age with 93-97.4% of the variation based on femoral diameter (with rather large 95% prediction limits). Together, when both variables (age and femoral diameter) were applied, they accounted for 97.7% of the total variation; but as with femoral diameter, the 95% confidence interval was still significant (Scuilli and Pfau, 1994: 1286). The authors posit that while the model was able to account for a large percentage of the total variation in the sample, 95% confidence interval was too wide to prove useful in estimating body mass.

Much like his 1991 study, Ruff (2007) used femoral distal metaphyseal and head breadths of radiographs of juveniles from a subset of the Denver Growth Study sample to produce body mass prediction equations for 20 individuals ages 1-17 years. For the older adolescents, body mass was also estimated from bi-iliac breadths and maximum length of the femur, tibia, humerus, and radius. Concerning his previous work in this methodology, Ruff found that when this method was applied to juveniles, it yielded prediction errors that were equal to or lesser than those created for adult body mass estimation. He found that body mass estimation was most accurate for individuals aged 2-7 years with a percent standard error estimate of about 5-6%. Additionally, this study found that at the ages where femoral head breadth was able to be assessed, it produced smaller associated errors than the distal metaphyseal breadth on average (Ruff, 2007:704).

To account for obese or underweight outliers present in many of the samples analyzed above, Moore (2008) collected measurements taken from CT imaging of 150 individuals from the William M. Bass Donated Skeletal Collection from the Department of Anthropology at the University of Tennessee-Knoxville. Using CT imagery, Moore (ibid.) was able to examine the cross-sectional geometry of the element in question, as well as the total cross-sectional area, second moment of inertia, second moment of area, polar moment of area, and centroid (center of cortical area). Analysis of these data revealed the strongest correlation in body mass for females was the proximal cortical area (R-squared = 0.62) and minimum moment of inertia at the proximal shaft (R-squared= 0.59). For males, the strongest correlation was from the principal moment of inertia at midshaft (R-squared = 0.59). Regarding the accuracy of the regression equations produced from these measurements, Moore (ibid: 63) stated that "…the multiple regression equations combining only the selected cross-sectional variables are not extremely strong for males or females". This study showed that body mass estimations are more accurate when multiple traits are combined, accounting for 60% of the variation in the sample (ibid: 62).

The research conducted by Elliot et al. (2015) is especially useful when considering the current practices of body mass estimation from postcranial variables as it applies the "most used" body mass estimation equations to a population of 253 individuals of known body mass. The sample consisted of CT imagery of 125 females and 128 males between the ages of 18 and 90 years obtained from the Institute of Forensic Medicine at the University of Zurich. While the different methods of body mass estimation often employ a variety of different measurements, this study focuses on the measurements of the biomechanical method of femoral head breadth as in Ruff et al. (1991; 1997; 2012), McHenry (1992), and Grine et al. (1995). This study found that, in reference to biomechanical methods for their sample, the mean percent prediction error (%PE) for Ruff's (1991) male-specific equations was 16.1% and estimated 71.1% of the male individuals ±20% of their body mass. Ruff's female equations yielded a %PE of 19% but estimated 48% of the sample ±20% of their body mass. The McHenry (1992) equations for single and combined sex produced equations for an estimated mass with a %PE below 19%, and above 50% of the individuals were estimated ±20% of their known mass. For morphometric body mass estimation methods, all equations applied resulted in estimates that fell within the criteria of the study which were deemed more reliable overall than their biomechanical counterparts as represented by a statistically significant p-value of $p<0.05$ (Elliot et al., 2015: 697).

Chapter 3: Materials and Methods

The USS Oklahoma Sample

The sample that was utilized for this study is the skeletal remains from US military personnel who died catastrophic deaths on the USS *Oklahoma* (BB-37) during the Japanese attack on Pearl Harbor on December 7, 1941. Catastrophic death referring to a death secondary to traumatic circumstances rather than an attritional death which would be secondary to some sort of pathology. In total, 429 individuals perished on the ship. 415 of these individuals were US Navy personnel and 14 US Marines (Brown, 2019). The day after the attack, recovery attempts began that continued for the following eight days until they were halted on December 16, 1941. Salvage attempts were resumed in July 1942 and continued until May 1944. Thirty-five individuals were identified in the years after the attack, but the remaining unidentified individuals were reinterred in various cemeteries as “unknowns”. The remains of these unknowns remained interred for two years before the American Graves Restoration Service (AGRS) exhumed all unknown remains in 1947. The remains were brought to the Central Identification Laboratory at Schofield Barracks for attempted identification. During this time, due to the possibility of the remains being interred as a group assemblage, the unassociated remains were sorted by element to inter the remains in as few caskets as possible. After this possibility was denied, Dr. Mildred Trotter directed the segregation of remains into individuals based on articulation, size, color, morphology, and texture. While Dr. Trotter recommended the identification of 27 individuals from the assemblage, they were not approved for identification due to the possibility of additional skeletal portions being present in the commingled assemblage. The remains were subsequently interred in the National Memorial Cemetery of the Pacific (NMCP) (Brown, 2019).

After being prompted by the research of a Pearl Harbor survivor, Mr. Ray Emory, one casket was disinterred from NMCP in 2003 by the Joint POW/MIA Accounting Command (JPAC) – a precursory institution of the current DPAA - for identification based on unique cranial/mandibular features identified by Trotter. Between the time of the first casket's disinterment from the NMCP and April 14, 2015, another single casket was disinterred, and extensive DNA testing was performed on the 200 associated elements. On April 14, 2015, the Deputy Secretary of Defense approved the exhumation of the remaining USS *Oklahoma* unknowns for large-scale identification between two DPAA laboratories in Hawaii and Nebraska along with the Armed Forces DNA Identification Laboratory (AFDIL) on Dover Air Force Base, Delaware (Brown, 2019: 102-105). As of September 30, 2019, the DPAA has positively identified 227 of the 388 remaining unknowns (Brown, 2019).

The measurements required to conduct this research were collected from a series of CT scans taken at the DPAA (Table 1, Figure 1). While the original sample consisted of 80 right and left femora from various individuals, three were excluded due to pathology that inhibited measurement and five additional femora were excluded because no antemortem body mass could be located for those individuals. Additionally, the sample was comprised of both paired elements (where both right and left femora have been matched via DNA, pair matching, and articulation analysis, to an individual) and single elements (where only one femur – right or left – has been associated an individual). So as to avoid multicollinearity, although a positively identified individual may have bilateral femora, only one femur was included for each. Finally, one individual was excluded as the time since body mass measurement was an exponential outlier in the sample (<6000 days). The remaining sample consisted of 53 femora (n=53; left=40, right=13) from 53 separate positively identified individuals from the total USS *Oklahoma* population. Scans were collected during the years of 2016-2017 on GM LightSpeed Series Computed Tomography Scanner by several different CT-trained analysts from the DPAA.

Methods

Step Number	*Measurement*	*Description*
1	Diaphyseal proxy line	Proxy line drawn along the superoinferior axis of the bone bisecting the medullary cavity at midshaft, following the complete length of the bone, and recording the angle of the line produced (0-90°).
2	Neck Proxy line	Proxy line drawn along the axis of the femoral neck from the most superomedial point on the femoral head, along the midline of the femoral neck, and extending underneath the greater trochanter.
3	Femoral Head Breadth (HeadBD)	Maximum breadth of the femoral head at the angle perpendicular to the neck proxy line.
4	Femoral Neck Breadth (NeckBD)	Maximum breadth of the femoral neck at the angle perpendicular to the neck proxy line.
5	Two thirds distance of HeadBD inferior the lesser trochanter	A line drawn at a distance two thirds HeadBD inferior the most medial point of the lesser trochanter and parallel to the diaphyseal proxy line.
6	Shaft diameter at two thirds HeadBD inferior the lesser trochanter (ShaftD)	Diameter of the femoral shaft at two thirds HeadBD and perpendicular to the diaphyseal proxy line.
7	Medial subperiosteal cortical breadth	Breadth of the medial periosteal cortical bone at two thirds HeadBD and perpendicular the diaphyseal proxy line.
8	Lateral subperiosteal cortical breadth	Breadth of the lateral periosteal cortical bone at two thirds HeadBD and perpendicular the diaphyseal proxy line.

Table 1: A detailed compilation of the eight steps in the data collection methodology

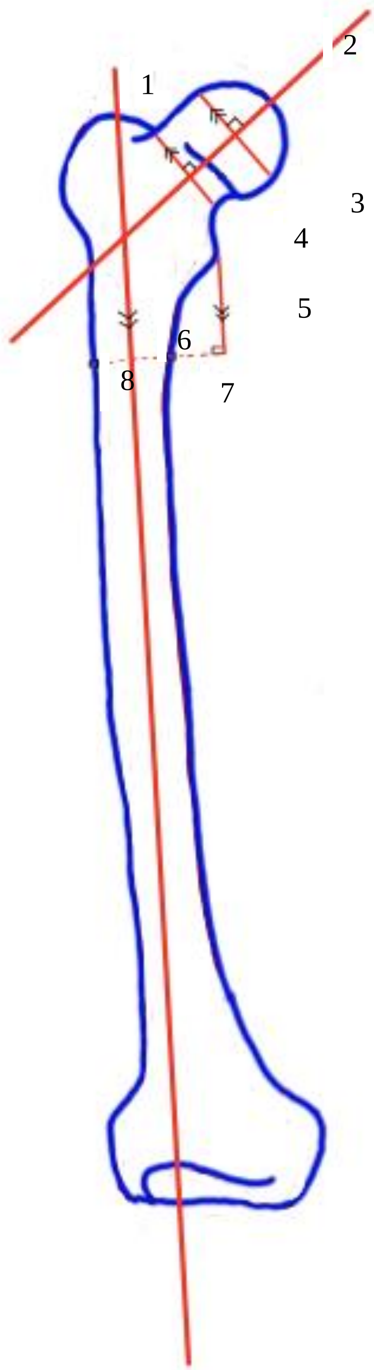

Figure 3: A graphic depicting the eight primary measurements in the data collection methodology.

In order to consistently collect the measurements mentioned in Ruff (1991) (femoral head breadth (HeadBD), neck breadth (NeckBD), shaft diameter (ShaftD), subperiosteal medial, and lateral cortical breadths), a detailed methodology was constructed utilizing the angles of two proxy lines drawn in the imagery along two axes of each femur in the sample. Per Ruff (1983), cortical area (CA) was calculated as it is proportional to the axial rigidity or strength of a long bone. While this is true, it is important to mention that the calculation for CA operates under the assumption that the element is symmetrical and circular in cross section, which of course is not the case.

$$CA = \pi/4 \cdot D^2 - d^2$$: D-subperiosteal diameter, d-medullary diameter

Measurements were collected from the anteroposterior scout image included with each CT scan using the software ImageWorks for Linux during the months of February and March 2019. In order to measure the accuracy of the body mass estimation method proposed by Ruff (1991) on this particular sample, reference masses (originally recorded in Lbs) were collected for each individual in the sample by accessing their Official Military Personnel File (OMPF) on record at the DPAA and documenting the body mass measurement taken closest to the date of death.

To collect the lines and measurements, the “measure” tool in ImageWorks was utilized. First, two proxy lines were drawn in order to measure the angle of the axis of the femoral diaphysis and femoral neck. Line 1 was drawn along the superoinferior axis of the bone bisecting the medullary cavity at midshaft, following the complete length of the bone, and recording the angle of the line produced (0-90°). Line 2 was drawn along the axis of the femoral neck from the most superomedial point on the femoral head, along the midline of the femoral neck, and extending underneath the greater trochanter. Like Measurement 1, the angle of this axis was recorded. Next, using the angle taken at Measurement 2, Measurement 3 was a collected via a perpendicular line (90°

measurement = degree of the perpendicular line) and the femoral head breath measurement was collected at the maximum diameter of the head at this angle. The femoral head measurement, just as femoral neck breadth and cortical breadths, was collected in millimeters. Referencing the angle used to take the Measurement 3, Measurement 4 was the femoral neck measurement collected at the minimum neck breadth along this same perpendicular angle.

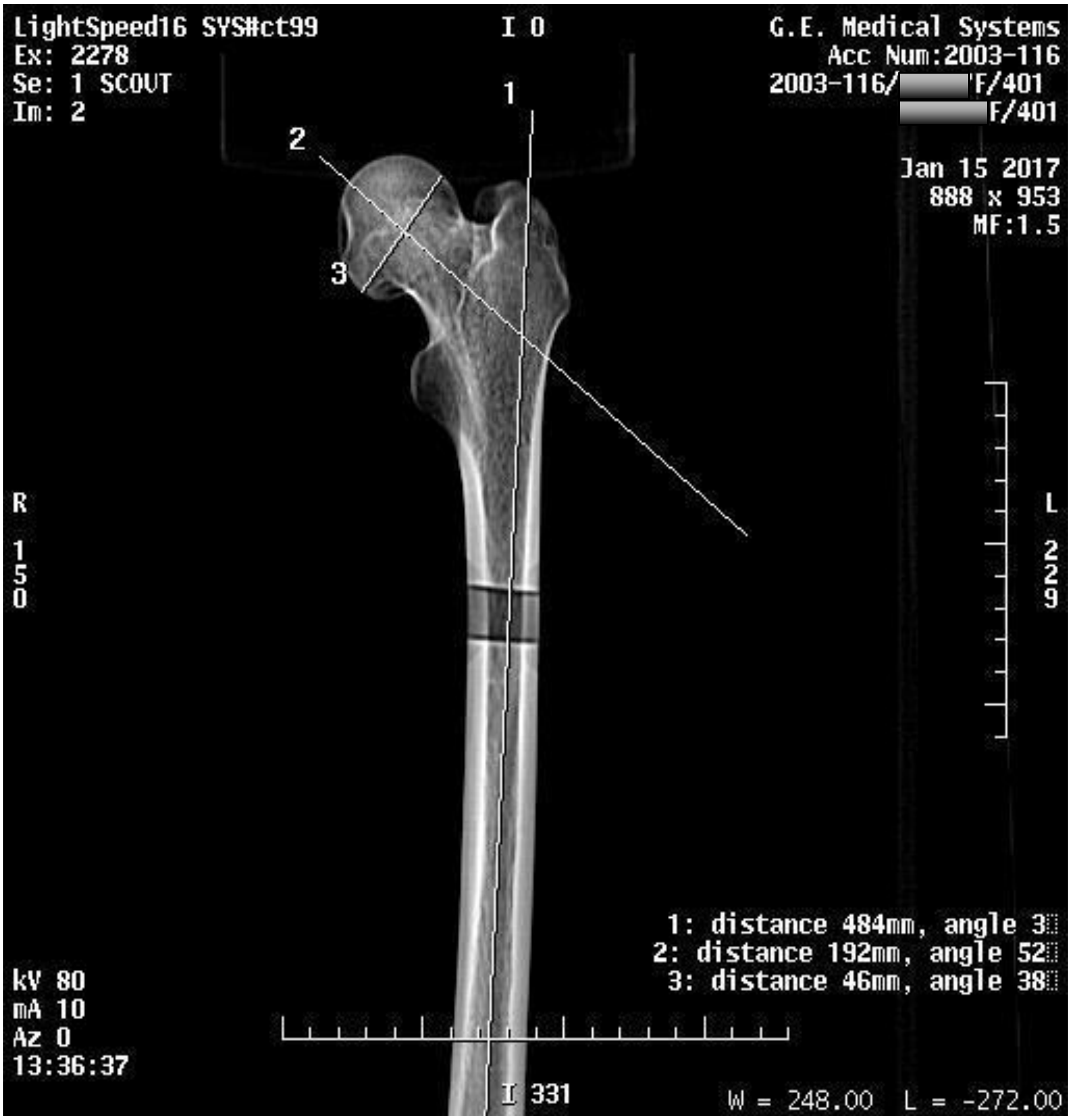

Figure 4: AP Radiograph of the proximal femur detailing measurements 1, 2, and 3. Line 1 is the superoinferior axis of the bone bisecting the medullary cavity at midshaft. Line 2 is the axis of the femoral neck from the most superomedial point on the femoral head. Line 3 is the measurement for femoral head breadth (HeadBD)

Figure 5: AP Radiograph of the proximal femur detailing measurement 4. This is the measurement of breadth taken at the femoral neck (NeckBD)

The next measurements were taken referencing the angle of the proxy line drawn in measurement 1. From the midpoint of the medial aspect of the lesser trochanter, a line was drawn towards the inferior at two thirds the length of the femoral head Measurement 3 at the same angle of Measurement 1 (designated Measurement 5). After this, a line perpendicular to Measurement 1 was drawn and mediolateral shaft breath was collected (designated Measurement 6). After collecting this, Measurements 7 and 8 were the medial and lateral subperiosteal cortical breaths that were collected along the same line and at the same perpendicular angle to 1 at 2/3 femoral head Measurement 3.

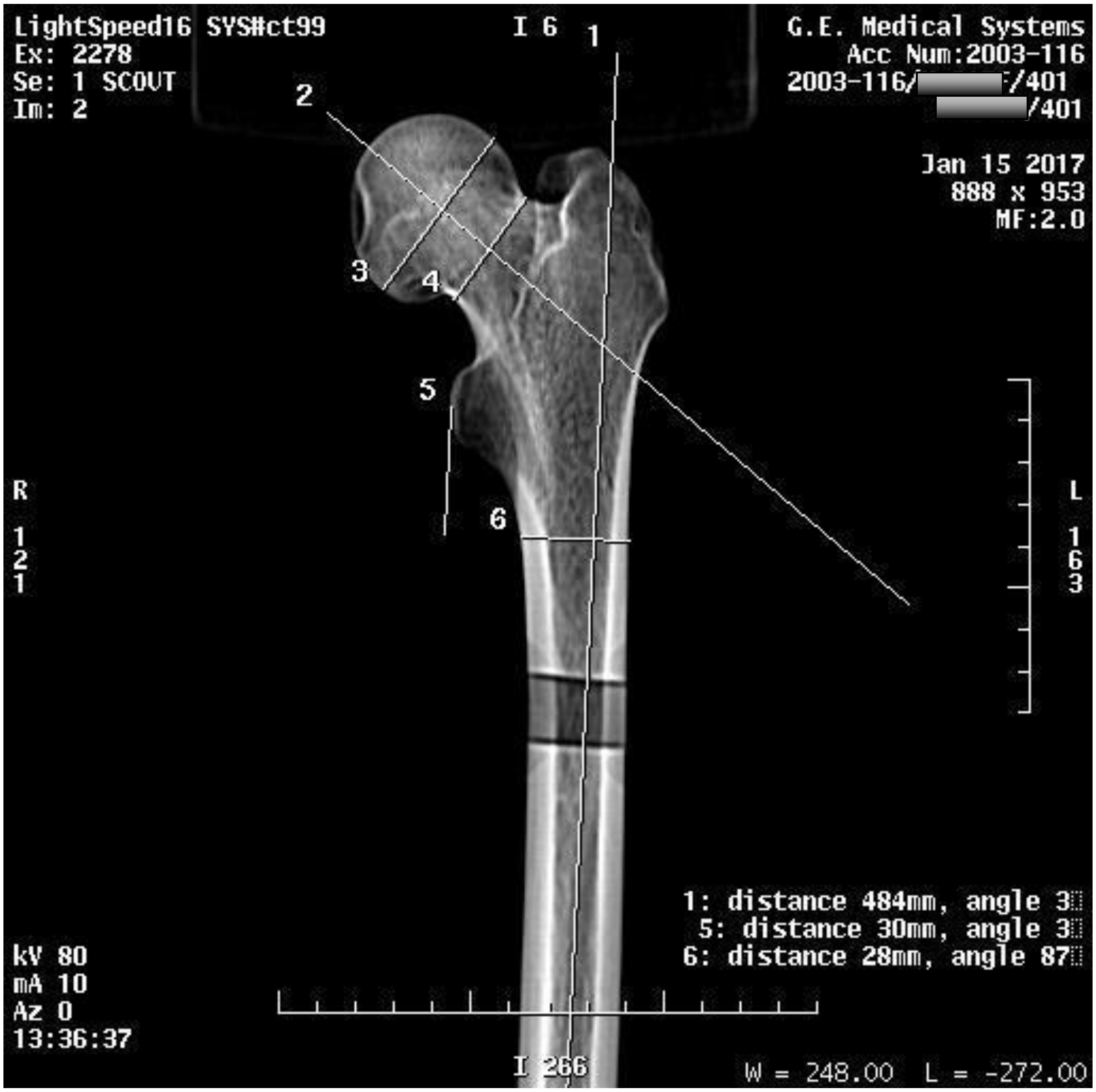

Figure 6: AP radiograph of the proximal femur detailing measurements 5 and 6. Measurement 5 was the measurement of ⅔ HeadBD and measurement 6 was Shaft BD.

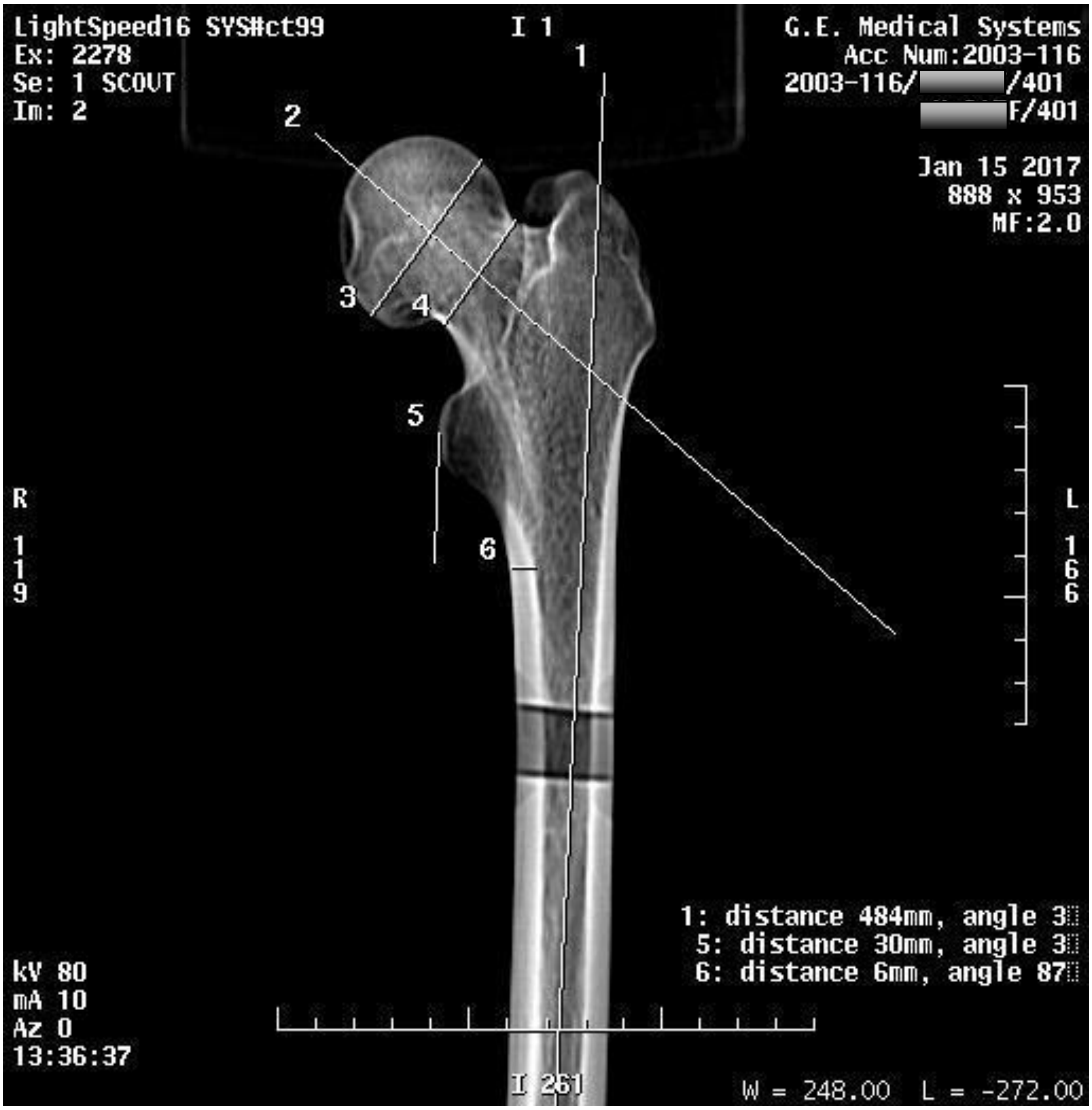

Figure 7: AP radiograph of the proximal femur detailing measurement 7. Number 6 in this figure measures medical cortical breadth

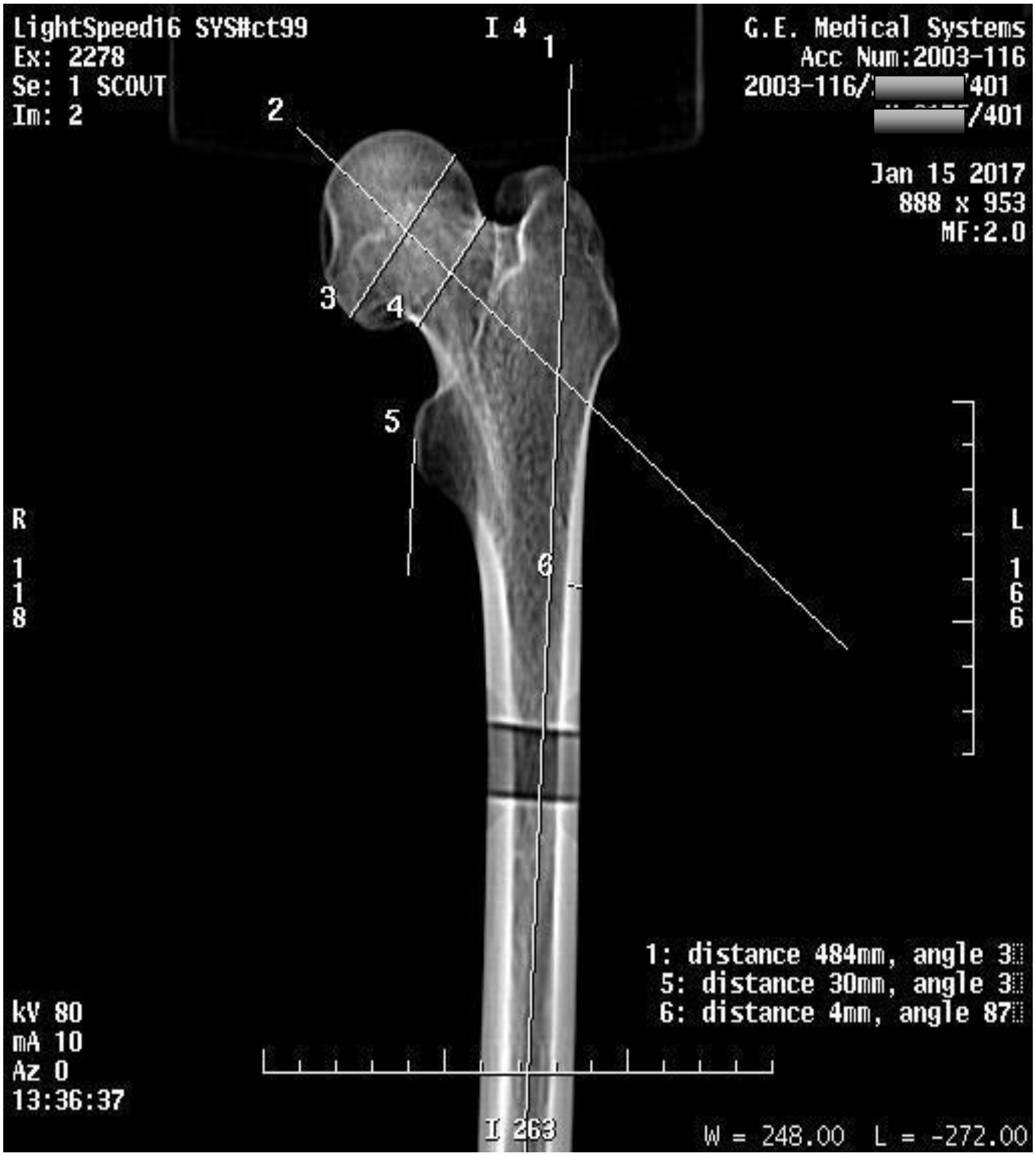

Figure 8: AP radiograph of the proximal femur detailing measurement 8. Number 6 in this figure represents lateral cortical breath

Chapter 4: Analysis

The data obtained from the USS *Oklahoma* is unique because the individuals were largely homogeneous (i.e., mostly comprised of young white males). This provides an opportunity to glean valuable insights into the relationship between antemortem weight and femur measurements, thus improving the ability to predict antemortem weight from postmortem data with more accuracy. The objective of this analysis is to determine the best method for predicting antemortem weight utilizing linear regression techniques and compare the results with previously established methods and models from Ruff (1991).

In order to gain a better initial understanding of the USS *Oklahoma* sample, descriptive statistics are obtained for the demographics of body mass, age, stature, and time since body mass measurement was collected from the individuals of whom the various femora belong (Table 2). The next step was to perform descriptive statistics on the applicable radiographic measurements taken from the CT data to understand the intrapopulation variation in the measurements. After these descriptive statistics were investigated, the observations with missing data due to taphonomical changes, trauma, and pathology were removed from the sample because the sample already includes sufficient data without missing values. Seven observations were removed, which resulted in a sample size of 53 femora. This type of analysis assumes that there is no variation in either the measurements being taken or biological variation in the sample. Linear regression modeling assumes the data follow the normal distribution [Kutner et al., 2013: 6]. Therefore, the distributions of each of the variables were checked, and all appear to be relatively normal (Figure 9).

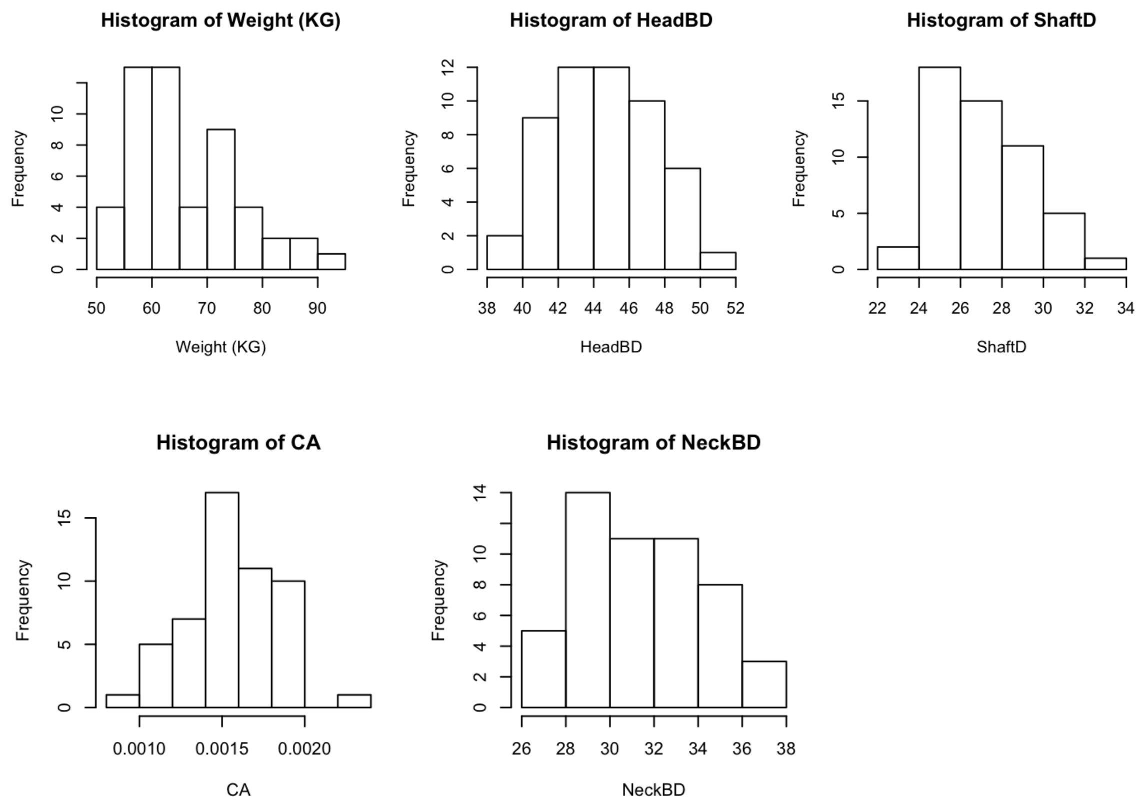

Figure 9: Distributions of the variables used for linear regression

Descriptive Statistics

All statistical analyses for this project were completed using R Version 3.5.2. In order to better understand the sample, descriptive statistics were conducted initially for the variables of body mass (kilograms – originally recorded in pounds), age (years), stature (inches), and time since the measurement was taken (days). The descriptive statistics for the sample (Table 2) included the mean, range (maximum/minimum), and standard deviation for all numerical variables in the sample (Teetor 2011: 276).

Following this, similar descriptive statistics were run for the measurements taken from the sample (Table 3). As mentioned above, the measurements were femoral Head Breadth (HeadBD), Neck BD (NeckBD), diaphyseal diameter at 2/3 the distance of HeadBD from the midpoint of the lesser trochanter (ShaftD), and CA. After assumptions were assessed, Pearson's correlation coefficients were then conducted to examine the linear relationship between the measurements taken and antemortem body mass in this sample. In order to compare the estimations yielded from the USS *Oklahoma* population to the estimations of Ruff (1991), the body mass measurements from the USS *Oklahoma* are presented in kilograms (kgs) instead of their original presentation of pounds.

	Body Mass (kgs)	Age (years)	Stature (in)	Time Since Measurement (Days)
Minimum	50.35	18	64	63
Maximum	90.72	43	74.5	3811
Mean	66.15	25	67.86	1067

Table 2: Descriptive Statistics for USS *Oklahoma* Sample

	HeadBD (mm)	NeckBD (mm)	ShaftD (mm)	CA (mm)
Minimum	38	26	22	.00098
Maximum	52	38	34	.0022
Mean	45.19	31.56	27.56	.0016
Std Deviation	2.84	2.70	2.15	.00026
Correlation Coefficient	0.428	0.272	0.639	-0.511

Table 3: Descriptive Statistics for Measurements Taken. Correlation Coefficient assessed in relation to antemortem body mass.

Comparison to Ruff's (1991) Body Mass Estimation Equations

In his 1991 study Ruff assessed the accuracy of his estimation equations through his calculation of both SEE and %SEE. These calculations were completed on the USS *Oklahoma* sample along with an additional calculation of MSE. As a manner of comparison, the antemortem body mass estimation equations offered in Ruff (1991) for White males were applied to this sample and the MSE was assessed and compared to the MSEs produced in this study. The MSEs produced from Ruff's (1991) equations were 104.12 and 62.50 for HeadBD and ShaftD, respectively. This differs from the MSE generated from the USS *Oklahoma* sample which were 81.85 and 59.99 for the same variables. Along with MSE, %PE and SEE was collected as means of comparison. Just as in Ruff (1991: 401), estimations taken from the femoral shaft tend to be more accurate on average than those taken from the femoral head. This conclusion is further outlined when looking at the SEE's of Ruff's (1991:406) equations for white males, 16.9 and 16.5 for

HeadBD and ShaftD compared to the USS *Oklahoma* sample that yielded SEE of 10.44 and 8.82 for the same demographic. To better visualize the differences in the models produced in Ruff (1991) and the USS *Oklahoma* data, the slopes for each equation were plotted against the collected measurements for HeadBD and ShaftD (Figures 8 and 9).

While Ruff (1991) included body mass estimation equations based on an idealized measurement of cortical area that assumes circularity of the transverse cross-section of the diaphysis at two thirds HeadBD, this was not included in the present study as the models were too dissimilar for comparison (i.e. lines of best fit were too dissimilar). This could be due to error in the calculation of cortical area based on the equation offered in Ruff (1991: 400) or possibly due to the demographic differences between Ruff's (1991) sample and the USS *Oklahoma* sample. While this is expected as the equations from the present study were fit to this specific set of data, the accuracy of the measurements and the clear differences in the lines of Ruff's sample are certainly notable. Additionally, just as in Ruff (1991: 401), estimations taken from the femoral shaft tended to be more accurate on average than those taken from the femoral head in the USS *Oklahoma* sample.

Analysis of Bilateral Sides

While only one femur was included per individual in the study, because the collected sample of femora were comprised of bilateral elements, further investigation analyses were completed to visualize whether side was significantly related to the collected measurements. To begin, interaction plots are used to assess whether the effects of variables, in this case side, change with respect to body mass. These interaction plots were examined to assess the data when grouped into sides against the collected variables of HeadBD, ShaftD, NeckBD, and CA (Figure 15). Overall, the plots show that there were no strong interactions between these variables and side. After these plots were examined, a model was fit to examine the multivariate relationship between side as a variable, the collected measurements (HeadBD, ShaftD, NeckBD, CA), and the antemortem body masses of the USS *Oklahoma* sample individuals. Using this model, VIF's were again calculated to test for multicollinearity. These results support that multicollinearity is not present in the model. The results are presented in Table 7 which report that sidedness is not significant when generating the models based on the measurements collected.

Simple Linear Regression and Body Mass Estimation

Because the variables that exhibited the highest level of correlation to antemortem body mass in Ruff's (1991) study were HeadBD and ShaftD, this analysis began with simple ordinary least squares linear regression models with each of these variables. However, before fitting regression models, it was important to review the assumptions behind linear regression modeling. According to Kutner et al. (2013), ordinary least squares regression assumes the variables are independent, normally distributed, and that the resulting model has constant residuals, normal error terms that sum to zero, and that multicollinearity does not exist (multiple linear regression). Inferences can be made only after these assumptions are met and verified. The normality of the variables was already checked as part of the initial data investigation; the histograms are found in Figure 9.

First, the resulting regression model with HeadBD as the independent variable and body mass as the dependent variable resulted in the regression equation:

Model 1: $\square_{\square} = 6.63 + 1.31\square_{1} + \square_{\square}$ - where $\square_{1}$ is HeadBD and $\square_{\square}$ is antemortem body mass

Before drawing inferences from this model, it is essential to check that the model was an appropriate fit to the data and make sure that any assumptions were satisfied. Figure 10 displays the model diagnostic plots for Equation 1. The residuals vs. fitted plot indicates that the residuals are relatively constant with respect to the fitted values. The Normal Q-Q plot (normal probability plot) shows that the residuals are relatively normally distributed and are relatively close to their respective theoretical quantiles. Additionally, the Scale-Location and Residuals vs. Leverage plots show there are no concerningly high leverage points or outliers. All of these plots confirmed that the model was a good fit for the data. The model was then interpreted; on average, with 1 millimeter (mm) increase in HeadBD, the antemortem body mass increases 1.31 kilograms. The intercept did not have any interpretable meaning here, because HeadBD would never equal zero. Figure 11 shows the USS *Oklahoma* data with the fitted regression model and the estimation equation yielded for Ruff's (1991) model of White males. Interestingly, Ruff's model is not included in the 95 percent confidence bands for the HeadBD Model, thus suggesting the two models are different from each other.

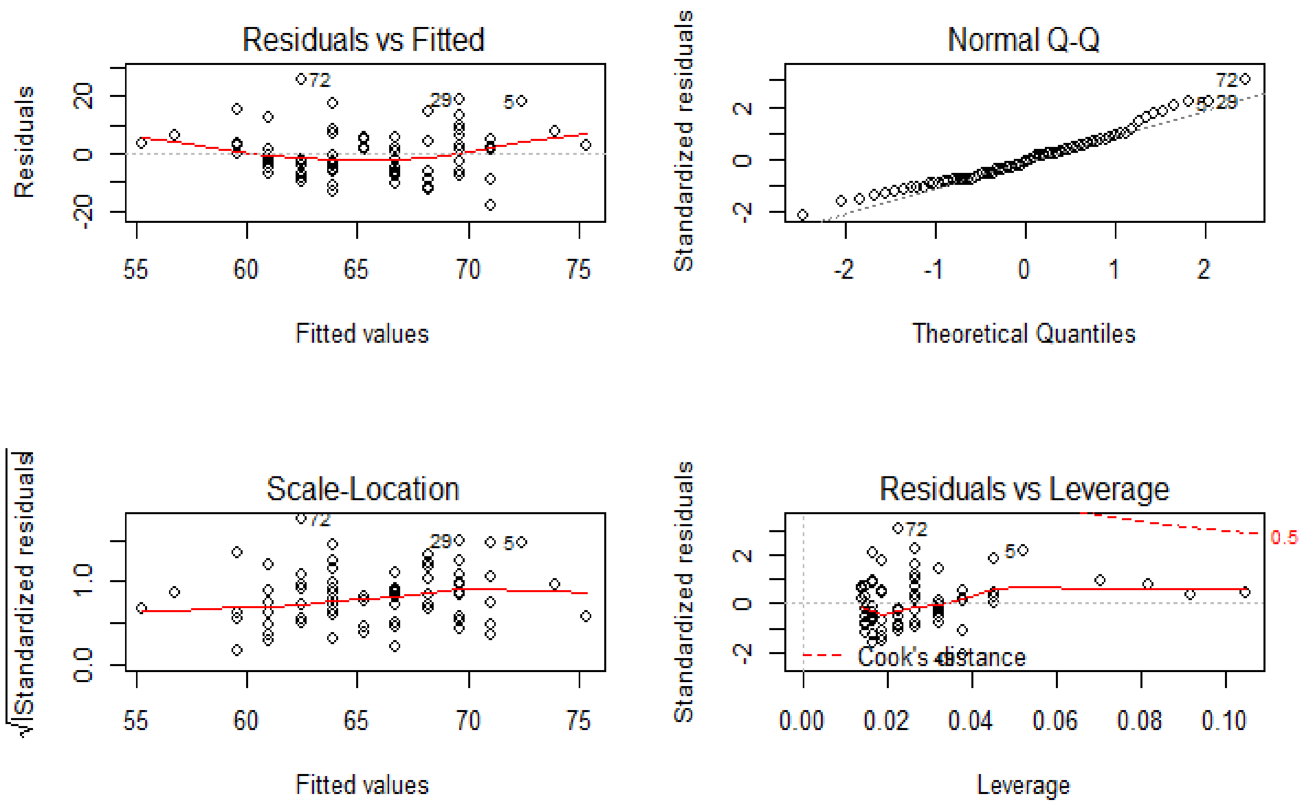

Figure 10: Model Diagnostic plots analyzing HeadBD Model

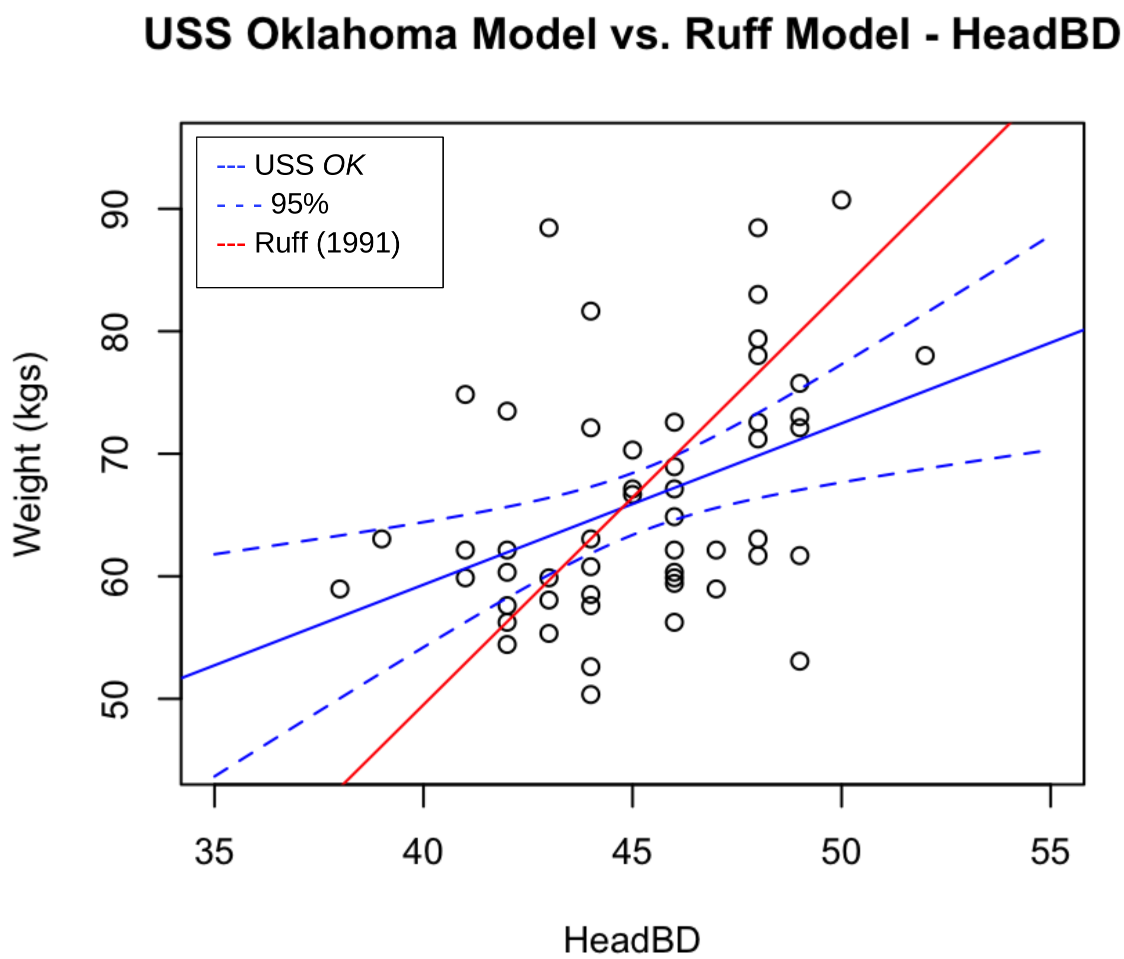

Figure 11: A plot visualizing the difference between the slope produced by Ruff's (1991) HeadBD data (red) and the USS *Oklahoma* HeadBD data (blue). A 95 percent confidence intervals was included for the USS *Oklahoma* model (dotted blue).

Next, the resulting regression model with ShaftD as the independent variable and body mass as the dependent variable resulted in the regression equation:

Model 2: $Y_i = -5.86 + 2.61X_1 + \epsilon_i$- where $X_1$is ShaftD and $Y_i$is antemortem body mass

The model diagnostic plots are shown in Figure 12. The Residuals vs. Fitted plot shows the residuals have relatively constant variance, the Normal Q-Q plot indicates the residuals are normally distributed, and the Scale-Location and Residuals vs. Leverage plots indicate no alarming high leverage points or outliers. Thus, the assumptions are met and the model parameters can be interpreted; on average, for one millimeter increase in ShaftD, the antemortem body mass increases 2.61 kilograms. Again, the intercept term does not have an applicable interpretation. Figure 13 shows Model 2 plotted with the USS *Oklahoma* data as well as Ruff's corresponding model. Interestingly, the majority of Ruff's model does fall within the 95% confidence bands of Model 2, which suggests the two models using ShaftD are fairly similar.

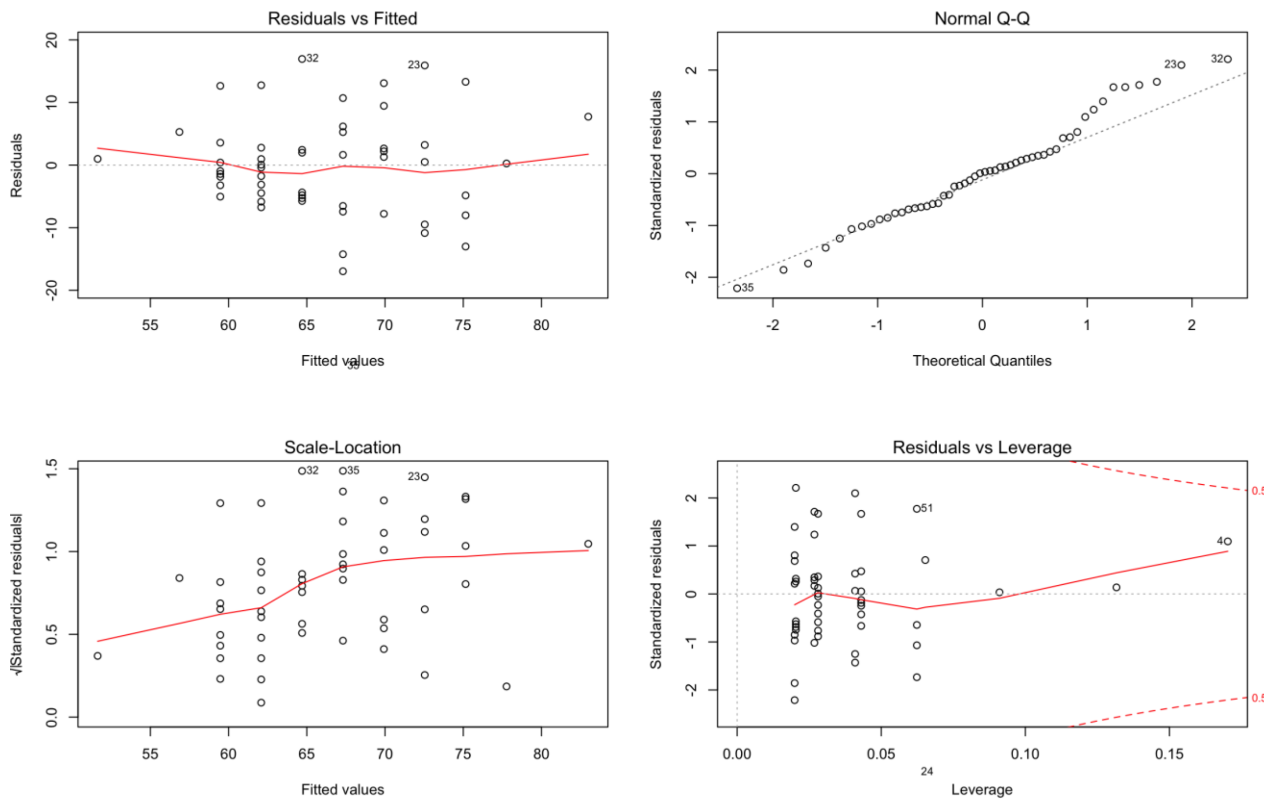

Figure 12: Model Diagnostic plots describing ShaftD Model.

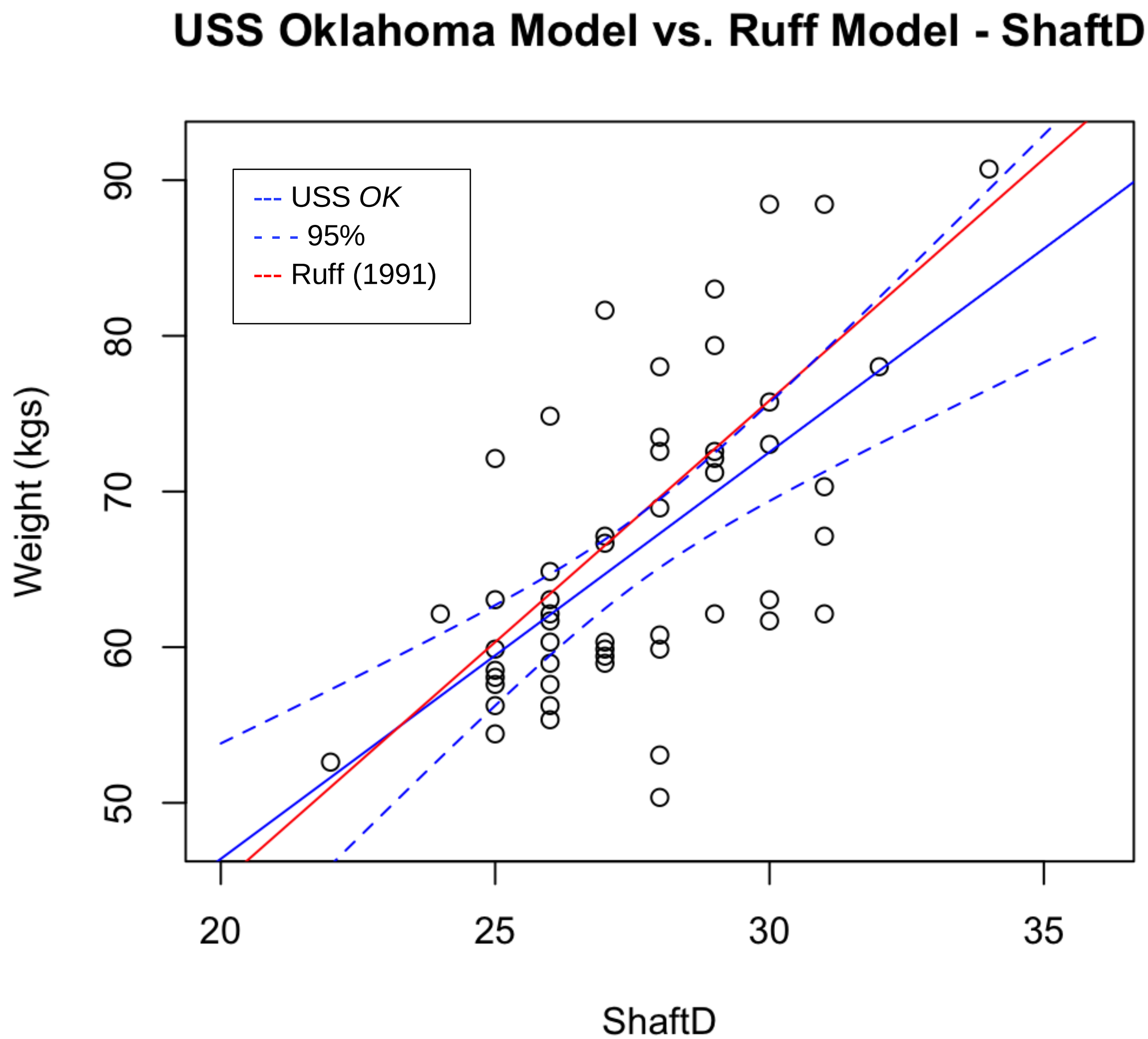

Figure 13: A plot visualizing the difference between the slope produced by Ruff's (1991) ShaftD data (red) and the USS *Oklahoma* ShaftD data. A 95 percent confidence intervals included for the USS *Oklahoma* model (dotted blue)

To assess the accuracy of the estimations yielded from the above equations, the correlations between HeadBD and antemortem body mass as well as ShaftD and antemortem body mass were examined (Table 4). For each measurement, R Values, Standard Error of Estimate (SEE), Absolute Percent Prediction Error |(%PE =

[(Observed-Predicted)/Predicted] · 100)| per Ruff (1991), Mean Squared Error (MSE), and Correlation Coefficient (p values) were calculated. Subsequently, comparisons were drawn to assess the variance that the simple linear models were able to account for. The coefficient of determination for HeadBD and ShaftD independently, when modeled against antemortem body mass, yielded values of R-squared= 0.14 and R-squared= 0.37, respectively. This result indicated that HeadBD was able to account for 14% of the variation in the sample while ShaftD accounted for 37%. In terms of correlation, the models yielded statistically significant (<.05) correlation values which are presented below. These correlation coeffects show that there is some relationship between the variable being assessed in the model and antemortem body mass. SEE was utilized to understand the fit of the model, as a larger SEE could mean that the data are not well explained with the simple linear relationship (Thomas, 1976: 362). After the results of this calculation confirmed the aptness of the models, %PE was calculated for comparability to the results offered in Ruff (1991). Mean squared error for the sample was calculated in order to assess the average squared difference between estimated body mass and actual body mass.

Validation of Simple Regression Models

In order to assess the applicability and usefulness of this model on outside datasets, the data was split in order to apply a Training and Test methodology. Per this method, a random sample of 80% of the ShaftD (the model that was able to account for the largest amount of variance – R-squared: .37) data were used as the training set from which a new linear model was created. Then, the remaining 20% of the data were applied to the model in order to test for overfitting of the data and to validate the original model. When completed, the method yielded MSE's of 46.003 and 32.9 for the training and test sets, respectively. In practice, these results validate the use of the ShaftD equation on outside data because the MSE for the test set is lower than that of the training set. This displays that the model generalizes to new data and is able to make new predictions without overfitting to the training set.

In order to understand the number of individuals that the model was able to correctly estimate within the 95% confidence interval, the upper and lower limits were calculated for the measurements present in the USS *Oklahoma* sample. Once this was completed, the antemortem body mass of each individual was compared to the upper and lower limits of the model for the respective measurements of HeadBD and ShaftD. In practice, the model for HeadBD was able to correctly estimate 32.0% (17/53) of the individuals in the sample within 95%. Similarly, the model for ShaftD was able to correctly estimate 34.0% (18/53) of the sample within a 95% confidence interval.

	R-squared	Adjusted R^2	SEE	%PE	MSE	p
HeadBD	.16	0.14	±8.87	±10.44	81.85	0.003
ShaftD	0.38	0.37	±7.60	±8.82	59.99	<0.001

Table 4: Results of Body Mass Estimation Equations

Multiple Linear Regression Analysis

After the variables collected had been assessed individually against the antemortem body mass data using simple linear regression, a multiple linear regression model was fitted with the variables of HeadBD, ShaftD, NeckBD, and CA in order to determine if the model could be improved (Teetor, 2011: 270). After the model was fit, residuals were assessed (Figure 14) and an ANOVA table was generated. The Residuals vs. Fitted plot shows the residuals again have relatively constant variance, the Normal Q-Q plot indicates the residuals are normally distributed, and the Scale-Location and Residuals vs. Leverage plots indicate the possibility of a relatively high, but still usable (within 0.5 limits) leverage point. Thus, the assumptions are still met and the model parameters can again be interpreted. Following the ANOVA, the model was assessed for multicollinearity through the calculation of the variance inflation factor (VIF) as it provides a quantification of the severity of multicollinearity in the regression analysis (Kutner et al., 2013: 408). The results produced from the ANOVA test and VIF calculation are presented in table 5 (Teetor 2011: 302).

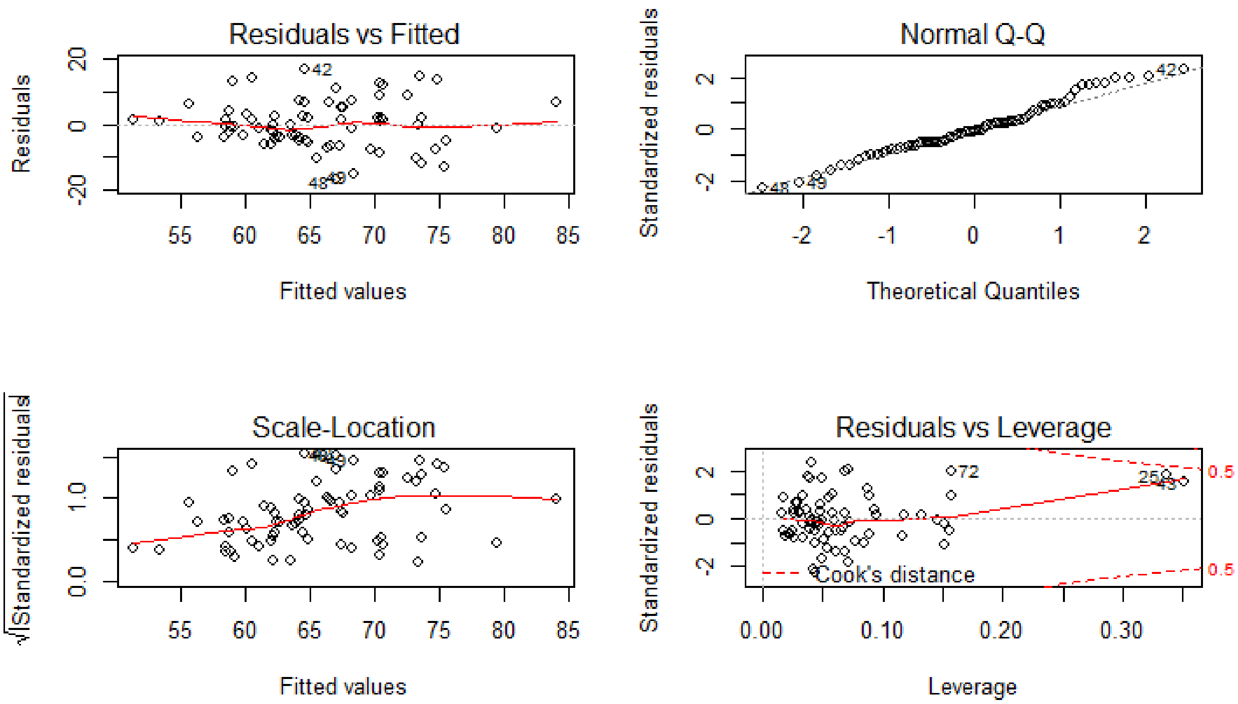

Figure 14: Model Diagnostic plots describing Multivariate Linear Regression Model

	Degrees of Freedom	Sum of Squares	Mean Sum of Squares	F-statistic	P-value	VIF
HeadBD	1	784.05	784.05	12.36	<0.001	1.76
ShaftD	1	1095.68	1095.68	17.28	<0.001	3.43
NeckBD	1	13.86	13.86	0.22	0.642	1.56
CA	1	3.59	3.59	0.06	0.813	2.80
Residuals	47	2979.58	63.40			

Table 5: Results of one-way ANOVA test with VIF for the multiple regression model.

After these variables were analyzed and VIF values were all under the threshold of 10 (hereby indicating no presence of multicollinearity (Kutner et al., 2013: 409), an interaction model was created to assess the possibility of non-causal relationships between the variables collected. In short, this was completed to understand if any single variable is driving the results of the other. The summary statistics produced by this model are presented in Table 6 These results inform that when all variables are included in the model and their interactions, no significant relationships exist to antemortem body mass. Additionally, these non-significant P values posit that when all these relationships are regressed together, the variables and interactions are not significantly related to the USS *Oklahoma* body mass data.

```
Residuals:
    Min      1Q  Median      3Q     Max 
-13.149  -4.412  -1.078   3.321  19.888 
Coefficients:
                Estimate Std. Error t value Pr(>|t|)
(Intercept)    3.615e+02  5.859e+02   0.617    0.541
headBD        -9.168e+00  2.064e+01  -0.444    0.659
shaftD        -6.457e+00  1.679e+01  -0.384    0.703
neckBD         2.683e-01  1.839e+01   0.015    0.988
CA            -3.932e+04  1.118e+05  -0.352    0.727
headBD:shaftD  3.237e-01  5.219e-01   0.620    0.539
headBD:neckBD -3.225e-02  2.075e-01  -0.155    0.877
headBD:CA      7.439e+02  4.072e+03   0.183    0.856
shaftD:neckBD -7.196e-02  4.966e-01  -0.145    0.885
shaftD:CA     -2.661e+03  2.191e+03  -1.215    0.231
neckBD:CA      2.344e+03  3.938e+03   0.595    0.555

Residual standard error: 8.093 on 41 degrees of freedom
Multiple R-squared:  0.4494,  Adjusted R-squared:  0.3151
F-statistic: 3.346 on 10 and 41 DF,  p-value: 0.002927
```

Table 6: Summary Statistics for Interaction Model.

<u>*Analysis of the Effects of Time*</u>

The next variable that was analyzed in this analysis was that of time since each individual's body mass data were collected. The time variable is defined as the number of days between death and the last body mass measurement taken while the individual was living. Because a larger amount of time since measurement could mean a less precise measurement due to body mass changes secondary to factors such as fitness regiments. The correlation coefficient between body mass and time is 0.17, which confirms that there could be a relationship between these two variables that may have an effect on the model. Because of this, a simple linear regression model was fit with time as the only independent variable. This model resulted in an R-squared value of only 0.009. This value confirms that time were no strong intravariable relationships when assessed individually. However, this variable may be useful in the final multivariate model, and thus was included below.

Application and Final Multivariate Model

As the initial multiple linear regression model did not have any significant variables, the final model included all the previously used variables, which included time and side (as a categorical variable). Then, the insignificant variables based on their p-values were removed until only statistically significant variables remained (alpha value 0.05). These variables were, NeckBD, CA, HeadBD. In order to test the statistical significance of side in the model, a generalized F test (Kutner et al., 2013: 72) was conducted with a full model that included HeadBD, ShaftD, side, and time, and the reduced model included HeadBD, ShaftD, and time. This test resulted in a p-value of 0.30, which is above any reasonable cutoff alpha value. Thus, the conclusion of this test is that side is not a significant predictor of body mass in this data and can be excluded from the model. This is pertinent to the study because not only does it allow for the use of right and left femora for this sample, it supports the application of this method to bilateral femora on outside samples of WWII era American White Males.

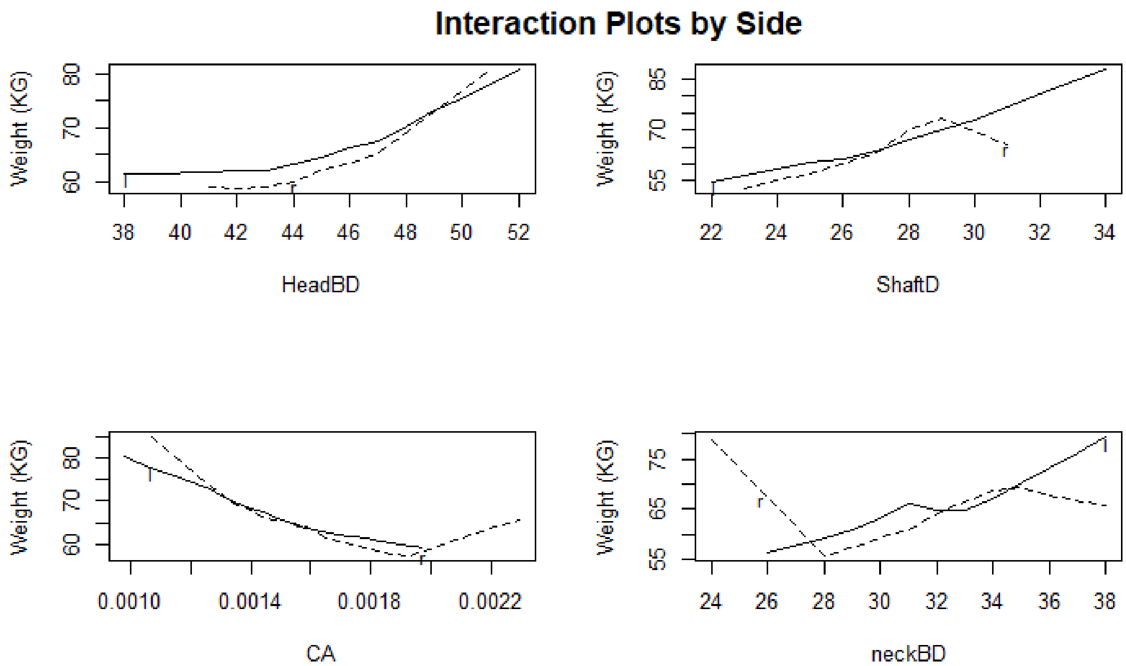

Figure 15: Interaction plots between side and the variable measurements collected.

Here, the final model consists of the two most significant variables, Time and ShaftD, which resulted in an R-squared value of 0.44 and an adjusted R-squared value of 0.42. VIF's produced from this model were 1.00, and this is because there were only two independent variables used in the model. Interpreting the coefficients, when X_2 – Time is held constant, and X_1 – ShaftD is increased by 1, antemortem body mass will increase by 2.71kg; similarly, when ShaftD is held constant and Time is increased by 1, body mass will increase by 0.002.

Final Model: $Y_i = -14.5 + 2.71X_1 + 0.002X_2 + \epsilon_i$ - where X_1 is ShaftD, X_2 is time and Y_i is antemortem body mass

```
Residuals:
    Min      1Q  Median      3Q     Max 
-18.971  -4.360  -0.545   4.633  19.365 

Coefficients:
                   Estimate Std. Error t value Pr(>|t|)    
(Intercept)      -12.483204  12.867782  -0.970   0.3369    
shaftD             2.776522   0.462273   6.006 2.45e-07 ***
as.factor(side)  -1.879812   2.452395  -0.767   0.4471    
time               0.002432   0.001082   2.248   0.0292 *  
---
Signif. codes:  0 ‘***’ 0.001 ‘**’ 0.01 ‘*’ 0.05 ‘.’ 0.1 ‘ ’ 1

Residual standard error: 7.5 on 48 degrees of freedom
Multiple R-squared:  0.4463,  Adjusted R-squared:  0.4117 
F-statistic:  12.9 on 3 and 48 DF,  p-value: 2.648e-06
```

Table 7: Summary of Final Multivariate Model

Validation Set with Final Multivariate Model

Finally, the final model was used with a validation procedure to test whether the model generalizes to new data and makes reasonable predictions. To do this, as above, the data was split into two groups, a training set and a testing set (80/20% randomized split). Then the final model consisting of ShaftD and time was fit using only the training data, before making predictions with the test data. The MSE was calculated for the model fit with the training set and the new predictions for the test set. The resulting MSE’s were 51.69 and 43.10, respectively. As in the simple model, since the training MSE was larger than the test, model is not overfitting to the data it was trained with and generalizes well to make new predictions.

Chapter 5: Discussion and Conclusion

The results produced from this analysis shows that while it may be possible to predict body mass from the human skeleton, and that biomechanical body mass estimation is closely tied to the sample from which the model is created, there is still recalibration that must be done before these methods of body mass estimation are put to practice. This is evident by R squared values of less than .5 in all the models generated from this sample. Simply put, even though the USS *Oklahoma* sample was able to control for many of the factors that other samples could not, there is still a large amount of variance left unaccounted for. As discussed above, this variance could be due to many of the substantiating factors such as genetics that complicate the estimation of this aspect of the biological profile. To some extent, the accuracy of the estimations is influenced by individual characteristics of the sample such as diet, environment, pathology, hormone levels, etc.

While many aspects of this study yielded different results from those offered in Ruff (1991), this study highlights many of the problems with using 2D radiographic measurements of skeletal material for body mass estimation. It is important to highlight that both the present study as well as Ruff (1991) operates under the assumption that the femoral cross-sectional geometry is perfectly circular, which is of course not the case. By operating under this assumption, the study is not able to account for the differences in cross-sectional geometry present in an actual sample secondary to concepts such as the Utah Paradigm. It would reason that this accounts for some of the previously unaccounted variance. Perhaps it is for this reason why Moore (2008) was able to account for ~60% of variance when considering true cross-sectional geometry of an element by applying biomechanically relevant measurements taken from CT imaging.

The results of this study demonstrate that even if we can control for many of the variables that confound body mass, there are underlying variables that we still do not fully understand, which affect our estimates. One of the possible compounding factors, as mentioned above, could be the individual genetic makeup of every individual in the sample. Just as every individual is different, so is each skeletal element. Grossly, this variation could present itself as a difference in bicondylar angle, femoral head diameter, diaphyseal length, and subperiosteal cortical breadth. On a microscopic level, variation could occur in the bone's ability to remodel, bone mineral density (BMD), and skeletal porosity. Since there are so many different factors that can lead to variability both grossly and microscopically, perhaps it would be best for continued research to utilize radiology of living individuals, as many of these variables can be measured and could aid in the culmination of more appropriate samples.

One avenue of continued research could bypass the anteroposterior scouts of these CT scans and venture into the true cross-sectional geometry of the elements (Moore 2013). Due in part to the success yielded from Moore (2008), as well as the fact that biomechanical strain is multifaceted and difficult to assess mathematically, much more study should be done into these different factors. Particularly, the different reactionary moments to applied forces, and how the skeletal tissue responds on a micro- and macroscopic level. Should this kind of CT study be completed on living individuals, it would be interesting to see the different types of chemical changes the bone undergoes in response to stress. This type of study could be further explored through long term investigation of individuals who undergo routine manual labor to quantify how much skeletal cross-sectional remodeling patterns are based on physical activity as opposed to other factors such as genetics.

Along with the application of this model to the more holistic field of forensic anthropology, another avenue of study would be the differences seen between the femoral morphologies of soldiers and civilians. Since it has already been established that muscle mass acts on skeletal tissue differently than fat mass, it would be interesting to investigate the morphological differences between individuals that gain wait due to the addition of muscle compared to fat. Further study such as this could possibly allow methodologies such as this to be applied to similar era males of European ancestry in the civilian sector. This could also be one way to investigate that applicability of this study to modern populations.

Limiting Factors

One of the most crucial limiting factors to this study, as is common with all anthropological research, is that of sample size. The sample that was applied to this This is compounded by the fact that not all body mass measurements had been taken recently, as is outlined in the 'time since measurement' statistic. Although extreme outliers were accounted for and most American military personnel were subjected to some level of fitness regiment, there is a possibility for body mass fluctuation in the time after the last measurement prior to December 7, 1941. Due to the rigorous physical training (PT) undergone by military personal after their induction, it is highly likely that new inductees gained a substantial amount of muscle mass which would sequentially impact body mass.

This possibility could potentially impact the study because the fluctuation could lead to inaccuracy in the data from which the estimation equations were derived. In order to better understand this, one could isolate the individuals in the sample whose body mass measurement occurred within a confined time period, for instance - one year, and see if the model generated by these individuals yield more accurate estimates.

A factor in this study that could not be controlled for the angle that the CT scans were taken. If an element is canted anteroposteriorly or mediolaterally while the scan is taking place, this could influence the measurements taken from the CT data. Because the CT images had already been taken prior to this study, the precision of the measurements could have been affected. An additional limiting factor to this study would be the possibility of body mass fluctuation after the most recent body mass was recorded. Although the most recent body mass measurement was collected at every available opportunity, many of the body mass measurements were taken at the time the individual was inducted to the military. Another possible limiting factor to data collection deals with the collection of the physical CT scans by DPAA analysts. Because no interobserver error analysis was completed, there is a possibility that the scans taken could have been completed in a way that could affect the measurements collected to produce the research above.

Finally, while measurements were taken in order to complete a traditional validation study with 10 elements outside the original data pool, body mass information was not retrieved due to an issue of data accessibility and security clearance. This is the reason why a Training and Test methodology was completed in lieu of the more traditional method. Additionally, no inter or intraobserver reliability study was completed during the initial study. Both inter and intraobserver error need to be assessed prior to application to any outside samples.

Conclusion

Through the implementation of Ruff's (1991) biomechanical method of body mass estimation and its subsequent application to a unique sample of individuals who were killed on the USS *Oklahoma* during the bombing of Pearl Harbor in 1941, this research was first able to create simple linear regression models for two of the variables that were offered by Ruff. These USS *Oklahoma* models yielded more accurate SEE's than the comparison study and adjusted R-squared values of .14 and .38 for the variables of HeadBD and ShaftD, respectively. After the models were generated and analyzed, a Training and Test methodology was applied for the model with the highest R-squared (ShaftD) which yielded two separate MSE's of 46.003 and 32.9, respectively. Since the MSE proved to be lower for the test set than the training set, this supports the model's applicability to outside datasets. The results from the simple linear regression models were then compared to the linear regression model presented in Ruff (1991). The MSEs produced from Ruff's (1991) equations were 104.12 and 62.50 for HeadBD and ShaftD, which differed from the MSE generated from the USS *Oklahoma* sample which were 73.50 and 56.01 for the same variables.

Aside from application and comparison to Ruff (1991), multivariate analysis was utilized to understand the relationship between variables and to improve body mass estimates. The data were analyzed to investigate intravariable relationships via interaction model that showed there was no statically significant correlation between variables. Next, additional testing was completed for the variables of time and side. In order to justify the use of bilateral elements from an individual in the sample, interaction plots were used along with multiple linear regression and application of a generalized F test to prove side is not a significant predictor of body mass in this data and thus that either side could be included for an individual. In terms of time since last body mass measurement, a correlation coefficient of 0.17 demonstrates that time since measurement could be significant in the model, but an adjusted R-squared value of .009 demonstrates that time since measurement is not a related variable when used by itself. Finally, Through the utilization of a multivariate regression model that utilized the most statistically significant variables collected from the sample, the final model yielded adjusted an R-squared value of .41, meaning that the final multivariate estimation model was able to account for 41% of the variance present in the sample. Lastly, the Training and Test methodology was again completed for the multivariate model and resulting MSE's were 51.69 and 43.10, respectively to the training and test sets. Since these MSE's are relatively close to each other, this supports that the model is not overfitting to the data and that it generalizes well to make new predictions.

Because these equations were able to produce more precise estimates than Ruff (1991), this evidence supports the original hypothesis of this study: that the precision of estimates produced from biomechanical body mass estimation methods will be positively impacted through controlling for demographic variables such as age, sex, extreme body masses, and pathology; as well as the fact that all of the USS *Oklahoma* deaths were catastrophic rather than attritional. Additionally, the application of multiple linear regression analysis was able to positively impact the amount of variance accounted for of the USS *Oklahoma* sample.

Overall, while this research was able to produce a more precise measurement, the fact that nearly half of the sample's variance remains unaccounted for acts as proof that body mass and cross-sectional geometry are tied to other confounding variables that were not analyzed in this research. It also illuminates that there is much more investigation that must be done before the estimation of this aspect of the biological profile applied to forensic contexts. While this method of body mass estimation has proven more precise in predicting a DPAA sample of WWII era white males ages 18-35, the results of this study suggest that it is not suitable for DPAA casework at this time. In conclusion, future researchers may wish to collaborate with medical professionals and utilize multivariate analysis accounting for a femur's true cross-sectional geometry as a means to better understanding how body mass is affecting living individuals. Doing this may hopefully further the field of forensic anthropology by creating better means of estimating this useful aspect of the biological profile.

REFERENCES

Auerbach B. and Ruff C. 2004a. Human body mass estimation: comparison of ‘morphometric’ and ‘mechanical’ methods. American Journal of Physical Anthropology 125(4):331-342.

Baker P and Newman R. 1957. The use of bone weight for human identification. American Journal of Physical Anthropology 15(4):601-618.

Brown C. 2019. The USS *Oklahoma* Identification Project. Forensic Anthropology 2(2):102-112.

Chevalier, Tony, Jan Clarys, Philippe Lefevre, Jean-Pol Beauthier, Stephane Louryan, and Erik Cattrysse. 2018. Body Mass Prediction from Femoral Volume and Sixteen Other Femoral Variables in the Elderly: BMI and Adipose Tissue Effects. American Journal of Physical Anthropology 166(1):26-42.

Choi K. and Goldstein S. 1992. A comparison of the fatigue behavior of human trabecular and cortical bone tissue. Journal of Biomechanics 25(2):1371-1381.

Curry J. 2002. Bones. Princeton. Princeton University Press.

De Groote I and Humphrey L. 2011. Body Mass and Stature Estimation Based on the First Metatarsal in Humans. American Journal of Physical Anthropology 144(4):625–632.

Delson E, Terranova C, Jungers W, Sargis E, Jablonski N, and Dechow P. 2000. Body Mass in Cercopithecidae (Primates, Mammalia): Estimation and Scaling in Extinct and Extant Taxa. Anthropological Papers of The American Museum of Natural History.

DeWitte S and Stojanowski C. 2015. The Osteological Paradox 20 Years Later: Past Perspectives, Future Directions. Journal of Archaeological Research 23(4):397-450.

Eckstein, F, Faber, Mühlbauer R, Hohe J, Englmeier K, Reiser M, and Putz R. 2002. Functional Adaptation of Human Joints to Mechanical Stimuli. Osteoarthritis and Cartilage 10(1):44–50.

Elliott M, Kurki H, Weston D, and Collard M. 2016. Estimating Body Mass from Postcranial Variables: An Evaluation of Current Equations Using a Large Known-Mass Sample of Modern Humans. Archaeological and Anthropological Sciences 8(4):689–704.

Huxley A. 1992. Estimation of Antemortem Body Weight from the Talus.

Katzenberg M and Grauer A. 2018. Biological Anthropology of the Human Skeleton. Hoboken. John Wiley & Sons.

Ketcham R and Ryan T. 2004. Quantification and Visualization of Anisotropy in Trabecular Bone. Journal of Microscopy 213(2):158-171.

Kirchengast S, Peterson B, Hauser G, and Knogler W. 2001. Body Composition Characteristics Are Associated with the Bone Density of the Proximal Femur End in Middle- and Old-Aged Women and Men. Maturitas 39(2):133–145.

Kurki H, Ginter J, Stock J, and Pfeiffer S. 2010. Body Size Estimation of Small-Bodied Humans: Applicability of Current Methods. American Journal of Physical Anthropology 141(2):169–180.

Kutner M, Nachtsheim C, Neter J, Li W. 2013. Applied Linear Statistical Models. New York City. McGraw Hill Education.

Lieberman D, Devlin M, Pearson O. 2001. Articular Area Responses to Mechanical Loading: Effects of Exercise, Age, and Skeletal Location. American Journal of Physical Anthropology 116(4):266–277.

Lin J, Grampp S, Link T, Kothari M, Newitt D, Felsenberg D, and Majumdar S. 1999. Fractal Analysis of Proximal Femur Radiographs: Correlation with

Biomechanical Properties and Bone Mineral Density. Osteoporosis International 9(6):516–524.

Lorkiewicz-Muszyńska D, Przystańska A, Kociemba W, Sroka A, Rewekant A, Żaba C, and Paprzycki W. 2013. Body Mass Estimation in Modern Population Using Anthropometric Measurements from Computed Tomography. Forensic Science International 231(1):405.e1-405.e6.

May, TA. 1999. The Study of Bone Mineral Density as a Predictor of Body Mass in Modern Homo sapiens.

McHenry H. 1992. Body Size and Proportions in Early Hominids. American Journal of Physical Anthropology 87(4):407-431.

Moore M. 2008. Body Mass Estimation from the Human Skeleton.

Moore M. 2013. Function Morphology and Medical Imaging. In: Digangi E and Moore M, editor. Research Methods in Human Skeletal Biology. Oxford: Elsevier Inc. p 397–424.

Moore M and Schaefer E. 2011. A Comprehensive Regression Tree to Estimate Body Weight from the Skeleton. Journal of Forensic Sciences 56(5):1115–1122.

O'Neill M and Ruff C. 2004. Estimating Human Long Bone Cross-Sectional Geometric Properties: A Comparison of Noninvasive Methods. Journal of Human Evolution 47(4):221–235.

Pomeroy E and Stock J. 2012. Estimation of Stature and Body Mass from the Skeleton among Coastal and Mid-altitude Andean Populations. American Journal of Physical Anthropology 147(2):264–279.

Pria B and Dalla A. 2012. Biomechanical Characteristics of the Bone. Human Musculoskeletal Biomechanics, edited by Tarun Goswami. InTech.

Robbins G, Sciulli P, and Blatt S. 2010. Estimating Body Mass in Subadult Human Skeletons. American Journal of Physical Anthropology 143(1):146–50.

Ruff C. 2007. Body Size Prediction from Juvenile Skeletal Remains. American Journal of Physical Anthropology 133(1):698–716.

Ruff C. 2000a. Body Mass Prediction from Skeletal Frame Size in Elite Athletes. American Journal of Physical Anthropology 113(4):507–517.

Ruff C. 2000b. Body Size, Body Shape, and Long Bone Strength in Modern Humans. Journal of Human Evolution 38(2):269–290.

Ruff C and Hayes W. 1983a. Cross-sectional Geometry of Pecos Pueblo Femora and Tibiae—A Biomechanical Investigation: I. Method and General Patterns of Variation. American Journal of Physical Anthropology 60(3):359–381.

Ruff C and Hayes W. 1983b. Cross-sectional Geometry of Pecos Pueblo Femora and Tibiae—A Biomechanical Investigation: II. Sex, Age, and Side Differences. American Journal of Physical Anthropology 60(3):383–400.

Ruff C, Holt B, Sládek V, Berner M, Murphy W, zur Nedden D, Seidler H, and Recheis W. 2006. Body Size, Body Proportions, and Mobility in the Tyrolean 'Iceman.' Journal of Human Evolution 51(1):91–101.

Ruff C, Holt B, Niskanen M, Sladek V, Berner M, Garofalo E, Garvin H. 2015. Gradual Decline in Mobility with the Adoption of Food Production in Europe. Proceedings of the National Academy of Sciences 112(23):7147–7152.

Ruff C, Scott W, and Liu A. 1991. Articular and Diaphyseal Remodeling of the Proximal Femur with Changes in Body Mass in Adults. American Journal of Physical Anthropology 86(3):397–413.

Ruff C, Walker A, and Teaford M. 1989. Body Mass, Sexual Dimorphism and Femoral Proportions of Proconsul from Rusinga and Mfangano Islands, Kenya. Journal of Human Evolution 18(6):515–536.

Ruff C, Niskanen M, Junno J, and Jamison P. 2005. Body Mass Prediction from Stature and Bi-Iliac Breadth in Two High Latitude Populations, with Application to Earlier Higher Latitude Humans. Journal of Human Evolution 48(4):381-392.

Salanthe Jr E, Arangio G and Salanthe E. 1987. An Application of Beam Theory to Determine the Stress and Deformation of Long Bones. Biomechanics 22(3):189-199.

Schlecht S and Jepsen K. 2013. Functional Integration of Skeletal Traits: An Intraskeletal Assessment of Bone Size, Mineralization, and Volume Covariance. Bone 56(1):127–138.

Schiessl H, Frost B, and Jee. 1998. Estrogen and Bone-Muscle Strength and Mass Relationships. Bone 22(1):1-6.

Sciulli P and Pfau R. 1994. A Method for Estimating Weight in Children from Femoral Midshaft Diameter and Age. Journal of Forensic Science 39(5):1280–1286.

Sciulli P and Blatt S. 2008. Evaluation of Juvenile Stature and Body Mass Prediction. American Journal of Physical Anthropology 136(4):387–393.

Sedlin E and Hirsch C. 1966. Factors Affecting the Determination of the Physical Properties of Femoral Cortical Bone. Acta Orthopaedica Scandinavica 37(1):29–48.

Shaw C. 2010. ‘Putting Flesh Back onto the Bones?’ Can We Predict Soft Tissue Properties from Skeletal and Fossil Remains? Journal of Human Evolution 59(5):484–492.

Sichta T. 2000. The estimation of ante-mortem weight from adult human skeletal remains: An examination of the humerus and the femur.

Smith R. 2002. Estimation of Body Mass in Paleontology. Journal of Human Evolution 43(2):271–287.

Smith R and Jungers W. 1997. Body Mass in Comparative Primatology. Journal of Human Evolution 32(6):523–559.

Squyres N and Ruff C. 2015. Body Mass Estimation from Knee Breadth, with Application to Early Hominins. American Journal of Physical Anthropology 158(2)198–208.

Stubblefield P. 2004. Cranial Size in Relation to Body Mass and Skeletal Robusticity in Modern Humans.

Teetor P. 2011. R Cookbook. Sebastopol: *O'Reilly Media Inc*.

Trinkaus E and Ruff C. 1999. Diaphyseal Cross-Sectional Geometry of Near Eastern Middle Palaeolithic Humans: The Femur. Journal of Archaeological Science 26(4):409–424.

Trinkaus E and Ruff C. 2012. Femoral and Tibial Diaphyseal Cross-Sectional Geometry in Pleistocene Homo. Paleoanthropology 13-62.

Trotter M. 1949. Operations at Central Identification Laboratory.

White T, Black M, and Folkens P. 2012. Human Osteology. Cambridge: Elsevier Academic Press.